Loss of TLR2 Worsens Spontaneous Colitis in MDR1A Deficiency through Commensally Induced Pyroptosis

Birgit Ey,* Annette Eyking,* Magdalena Klepak,* Nita H. Salzman,[†] Joachim R. Göthert,[‡] Michael Rünzi,[§] Kurt W. Schmid,[¶] Guido Gerken,* Daniel K. Podolsky,[‖] and Elke Cario*

Variants of the multidrug resistance gene (*MDR1/ABCB1*) have been associated with increased susceptibility to severe ulcerative colitis (UC). In this study, we investigated the role of TLR/IL-1R signaling pathways including the common adaptor MyD88 in the pathogenesis of chronic colonic inflammation in MDR1A deficiency. Double- or triple-null mice lacking TLR2, MD-2, MyD88, and MDR1A were generated in the FVB/N background. Deletion of TLR2 in MDR1A deficiency resulted in fulminant pancolitis with early expansion of CD11b$^+$ myeloid cells and rapid shift toward TH1-dominant immune responses in the lamina propria. Colitis exacerbation in TLR2/MDR1A double-knockout mice required the unaltered commensal microbiota and the LPS coreceptor MD-2. Blockade of IL-1β activity by treatment with IL-1R antagonist (IL-1Ra; Anakinra) inhibited colitis acceleration in TLR2/MDR1A double deficiency; intestinal CD11b$^+$Ly6C$^+$-derived IL-1β production and inflammation entirely depended on MyD88. TLR2/MDR1A double-knockout CD11b$^+$ myeloid cells expressed MD-2/TLR4 and hyperresponded to nonpathogenic *Escherichia coli* or LPS with reactive oxygen species production and caspase-1 activation, leading to excessive cell death and release of proinflammatory IL-1β, consistent with pyroptosis. Inhibition of reactive oxygen species–mediated lysosome degradation suppressed LPS hyperresponsiveness. Finally, active UC in patients carrying the TLR2-R753Q and MDR1-C3435T polymorphisms was associated with increased nuclear expression of caspase-1 protein and cell death in areas of acute inflammation, compared with active UC patients without these variants. In conclusion, we show that the combined defect of two UC susceptibility genes, MDR1A and TLR2, sets the stage for spontaneous and uncontrolled colitis progression through MD-2 and IL-1R signaling via MyD88, and we identify commensally induced pyroptosis as a potential innate immune effector in severe UC pathogenesis. *The Journal of Immunology*, 2013, 190: 5676–5688.

Inflammatory bowel disease (IBD) is thought to result from inappropriate innate immune responses to commensal enteric bacteria (1, 2). Genetic predispositions may trigger procolitogenic perturbations of the host–commensal relationship. Alterations in intestinal epithelial cell (IEC) barrier function and antimicrobial defense mechanisms may lead to prolonged immune cell activation and impaired bacterial clearance (3), yet the dissection of most IBD susceptibility genes, especially their functional interaction and outcome, is still in its infancy. Specific single mutations linked to IBD may neither be necessary nor sufficient to cause disease. Both environmental factors and the interplay between variants at several contributing genetic loci may trigger development of disease and explain the phenotypic diversity of IBD. So far few studies have been undertaken to determine how the combination of distinct IBD-associated gene defects may influence phenotype.

Extensive and fulminant colonic disease affects up to 40% of the total human ulcerative colitis (UC) population and remains a therapeutic challenge. Variations of the multidrug resistance gene (*MDR1/ABCB1*) have been associated with increased susceptibility to severe UC (4, 5). Expression of MDR1 is reduced in the inflamed intestine of UC patients, which is associated with disease aggravation (6). Mice deficient in MDR1A develop spontaneous chronic colitis (7) that resembles human UC pancolitis (8): continuous inflammation of the entire colon and mucosal thickening with crypt abscesses and distortion. There is emerging evidence that MDR1A plays a critical role in host–bacterial interactions in the gastrointestinal tract and in the maintenance of intestinal homeostasis. P-glycoprotein, which is encoded by *MDR1A*, functions as an ATP-dependent efflux transporter pump of bacterial xenobiotics and toxins, as well as drugs (7, 9). Deletion of the *MDR1A* gene impairs the IEC barrier, allowing bacterial translocation to the underlying lamina propria (10–12). Systemic administration of a lipid A-mimetic has been shown to inhibit the development of chronic colitis in MDR1A-null mice (13). However, the innate immune mechanisms involved in modulating the

*Division of Gastroenterology and Hepatology, University Hospital Essen, University of Duisburg-Essen, 45122 Essen, Germany; [†]Division of Gastroenterology, Department of Pediatrics, Medical College of Wisconsin, Milwaukee, WI 53226; [‡]Division of Hematology, University Hospital Essen, University of Duisburg-Essen, 45122 Essen, Germany; [§]Division of Gastroenterology and Metabolic Diseases, Kliniken Essen Süd, 45239 Essen, Germany; [¶]Institute of Pathology and Neuropathology, University Hospital Essen, University of Duisburg-Essen, 45122 Essen, Germany; and [‖]Department of Internal Medicine, University of Texas Southwestern Medical Center, Dallas, TX 75390

inflammatory process in the context of MDR1A deficiency have not yet been delineated.

TLRs represent key mediators of innate host defense in the intestine (14). TLRs recognize ligands that can be classified into microbiota-/viral-associated and damage-associated molecular patterns. Ligand engagement induces conformational changes and interactions of TLRs with coreceptors that allow recruitment of adaptor proteins, such as MyD88 (15). Lipopeptide binding induces interaction of TLR2 with TLR1 (16), whereas MD-2 is the essential coreceptor of TLR4 for specific LPS recognition (17). In the intestinal mucosa, a defect in TLR signaling may influence ligand recognition and immune tolerance, leading to changes in innate and adaptive immune reactivity (14). Within a healthy host, TLR signaling drives basal immune mechanisms essential for protecting IEC barrier integrity and maintaining commensal tolerance. However, within a susceptible individual, aberrant TLR signaling may impair commensal–mucosal homeostasis, thus contributing to amplification of inflammation in IBD.

TLR2 loss of function by the heterozygous TLR2-R753Q polymorphism has previously been associated with a more severe disease phenotype in UC (18). Expression of TLR2-R753Q impairs IEC wound healing in vitro (12, 19). However, the role of TLR2 in colitis is still controversial. We have recently shown that TLR2 maintains functional tight- and gap-junction–associated barrier integrity and protects against apoptosis in the intestinal epithelial layer, thus ameliorating stress-induced mucosal damage in acute DSS colitis in wild-type (WT) mice and spontaneous chronic colitis in MDR1A knockout (KO) mice (12, 19, 20). Yet, in the setting of NOD2 deficiency, TLR2 may drive exaggerated proinflammatory TH1 responses in the model of T cell transfer colitis (21). In contrast, TLR2 seems to be dispensable for *Helicobacter hepaticus*–mediated intestinal inflammation (22).

In this article, we show that a combined defect of the two UC susceptibility genes, *MDR1A* and *TLR2*, sets the stage for spontaneous and uncontrolled colitis progression through MD-2 and IL-1R signaling via MyD88. We identify excessive pyroptosis as a maladaptive host defense strategy for clearance of commensal gut bacteria that contributes to the development of severe TH1-cytokine–mediated intestinal inflammation. Thus, our data imply a novel mechanistic link between aberrant innate immune signaling and microbial processing in the pathogenesis of severe chronic colitis.

Materials and Methods

Abs and reagents

CD11b, CD4, and CD8 Abs were from BD Pharmingen. CD45 Ab was from Santa Cruz, IL-1β Abs from R&D Systems and Abcam, IL-18 Ab from Abcam, COX IV and LAMP-1 Abs from Cell Signaling, caspase-1 Ab from Invitrogen, and ZO-1 Ab from Zymed. Alexa Fluor 488– and Alexa Fluor 647–conjugated goat anti-rabbit or anti-rat IgG Abs were from Invitrogen. HRP-conjugated anti-rabbit and anti-mouse Abs were from GE Healthcare, HRP-conjugated anti-goat Ab from ICN, and FITC-conjugated donkey anti-goat or CY5-conjugated goat anti-rabbit IgG Abs from Jackson Immunoresearch. Caspase-1 inhibitor IV (Ac-YVAD-AOM; which blocks specifically caspase-1 cleavage) (23) was from Merck. The reactive oxygen species (ROS) inhibitor diphenyleneiodonium chloride (DPI) (24) was from Enzo; chloroquine (CQ), an inhibitor of endosomal/lysosomal acidification (25), and glyburide (GB), an inhibitor of the NLPR3 inflammasome (26), were from InvivoGen. All other reagents were obtained from Sigma-Aldrich, unless otherwise specified.

Human colonic biopsies

Fresh colonic tissue samples from healthy and active UC patients undergoing colonoscopy were collected at the Division of Gastroenterology and Metabolic Diseases, Kliniken Essen Süd, Germany. Informed consent was obtained from all patients before the procedure, and the study was reviewed and approved by the Human Studies Committee of Kliniken Essen Süd. Patients with gastrointestinal infection were excluded. The colonic specimens were immediately immersed into RNA*later* (Ambion) and stored at −80°C until further processing. Parallel samples from each patient were pathologically reviewed.

Animals

WT FVB/N mice and parental MDR1A KO mice (7) (originally developed by Dr. Alfred Schinkel, The Netherlands Cancer Institute) were obtained from Taconic Farms (Germantown, NY) under crossbreeding agreement. TLR2 KO (B6.129-*Tlr2tm1Kir*/J; The Jackson Laboratory), MyD88 KO (20, 27) (provided by Dr. Shizuo Akira, Osaka University, Japan), and MD-2 KO (17) (provided by Dr. Kensuke Miyake, University of Tokyo, Japan) mice (all C57BL6/J) were backcrossed for seven generations onto MDR1A KO (FVB/N) mice and then bred as double-KO (dKO) homozygotes; control MDR1A KO or TLR2 KO mice were derived from the littermate F7-(FVB/N) generations; triple-KO (tKO) mice were obtained by subsequent intercrossing. All mice were (back)bred and housed in the same temperature- and humidity-controlled room (*Helicobacter/MNV*-free) on a 12-h light/dark cycle under strict specific pathogen-free conditions (Central Animal Facility, University Hospital Essen, Germany). The animals were provided with autoclaved tap water and autoclaved standard laboratory chow ad libitum. Extensive animal health monitoring was conducted routinely on sentinels and representative mice from this room. Mice were genotyped by PCR assay on genomic DNA isolated from tail clips. For studies, only male mice aged 5 and 10 wk old, or as indicated otherwise, were used. For microbiota analysis, successive litters of individual heterozygous breeding pairs were analyzed to control for maternal influence, as previously described (28). Protocols were in compliance with German law for use of live animals, and reviewed and approved by the Institutional Animal Care and Use Committee at the University Hospital Essen and the responsible district government.

Histologic evaluation of colitis

Frozen cross sections (7 μm) of murine distal colons or human colonic biopsies were stained with H&E (Fast Frozen Stain Kit; Polysciences). Histologic severity of colitis was assessed and scored in mice, as previously described (12). All slides were scored in a blinded fashion. Standardized images were obtained with an Eclipse E600 microscope (Nikon).

Commensal microbiota depletion

TLR2/MDR1A dKO mice were treated with either antibiotics in drinking water (vancomycin-imipenem [both 50 mg/kg body weight/d]) or water alone (as controls) for 8 wk in prophylaxis and therapy protocols. Prophylaxis started at the age of 3 wk directly after weaning and before the onset of colitis. Treatment was begun at 18 wk of age, when all mice had developed severe colitis. In combination, vancomycin and imipenem are broadly active against almost all aerobic and anaerobic bacterial species, and used for gut decontamination (29).

In vivo treatment with IL-1R antagonist

Starting at 5 wk of age, TLR2/MDR1A dKO mice were treated with IL-1R antagonist (IL-1Ra [Anakinra]; Kineret, Swedish Orphan Biovitrum) by once daily s.c. injection (100 mg/kg BW) for 28 d (30); controls received isotonic saline solution in parallel.

Murine cell isolation and stimulation

Bone marrow cells flushed from femurs and peripheral blood cells were isolated as described previously (31). Colonic lamina propria mononuclear cells were isolated as previously described (32) with minor modifications. In brief, colons were cut open longitudinally, washed with ice-cold HBSS, and digested with dispase (2 mg/ml; Life Technologies) at 37°C for 50 min in complete media (RPMI 1640 media supplemented with 4% FCS, 2.5% HEPES, 1% penicillin/streptomycin, and 1% antibiotic/antimycotic solution; PAA) to remove the epithelial compartment. Samples were then minced into small pieces and further digested with collagenase II (1.5 mg/ml; Life Technologies) and dispase (1.0 mg/ml) for 50 min at 37°C. For CD11b+ cell purification, cells were passed through a cell strainer (100 μm; BD Falcon) and purified using the EasySep CD11b Positive Selection Kit (Stemcell Technologies). For T cell purification, cells were passed through a glass wool column and purified via a 45%/72% Percoll gradient; the interface was further purified by negative selection using the EasySep Mouse T Cell Enrichment Kit (Stemcell Technologies). In all isolation protocols, enucleated RBCs were lysed with ammonium-chloride-potassium buffer. Peritoneal myeloid cells were isolated via lavage of the peritoneal cavity with culture medium and purified by cell adherence (0.2–1 × 10^6/well; 3 h) to poly-D-lysine–coated (BD BioCoat) tissue culture plastic or the EasySep CD11b Positive Selection Kit (CD11b+ purity > 95%). Myeloid

cells were stimulated with nonpathogenic, noninvasive *Escherichia coli*–enhanced GFP DH5 (provided by Dr. Cathryn Nagler) (33) for 90 min (at a ratio of 5:1 bacteria/cell) or ultrapure LPS *E. coli* serotype R515 (1 μg/ml; Alexis) for 23 h.

Flow cytometry analysis

After washing and incubation with FcR block (CD16/CD32), cells were analyzed using a BD LSRII (BD Biosciences) after staining with Ab mixtures: murine CD11b, Ly6C, Ly6G, F4/80, CD11c, and CD103. In some cases, cells were fixed for 15 min at room temperature (RT) in freshly prepared 4% paraformaldehyde and analyzed the next day. All Abs and appropriate isotype IgG controls were purchased from BD Biosciences, BioLegend, or eBioscience. The BD Cytofix/Cytoperm kit (BD Biosciences) was used for intracellular staining of IL-1β. Dead cells were excluded by staining with propidium iodide or LIVE/DEAD fixable dead cell stain kit (Invitrogen). Flow cytometry data were analyzed using FlowJo software for PC (version 7.6.5; Tree Star).

Phagocytosis assay

Phagocytosis of peritoneal myeloid cells was assessed through the uptake of *E. coli* particles labeled with a low pH-sensitive dye by flow cytometry within the CD11b-gate, according to the manufacturer's instructions (pHrodo *E. coli* bioparticles; Invitrogen).

Immunofluorescence

Frozen sections of tissues were cut (7 μm) and mounted on Superfrost Plus Gold slides (Thermo); cells were directly grown on coated culture slides. Dependent on primary Abs, sections were fixed with either acetone (100%) for 5 min at −20°C or methanol/acetone (50:50) for 5 min at −20°C followed by air-drying and washing. The sections were then blocked with normal goat or donkey serum (1:10 in PBS) for 60 min at RT and incubated with primary Abs (1:50–200) overnight at 4°C. Fluorescent-labeled Abs were used as secondary Abs (1:50–100, 60 min, RT). For intracellular ROS detection, cells were stained with CellROX Deep Red (Invitrogen), according to the manufacturer's instructions. After mounting with Vectashield Mounting Medium with propidium iodide or DAPI (Vector Laboratories), immunofluorescent sections were assessed by using a laser-scanning confocal microscope (Zeiss Axiovert 100M-LSM510; Carl Zeiss, Jena, Germany). The multitrack option of the microscope and sequential scanning for each channel were used to eliminate any cross talk of the chromophores. All images were captured under identical laser settings. Results were only considered significant if >80% of the scanned sections per field exhibited the observed effect; representative results are shown. Control experiments were performed with isotype control IgG (Santa Cruz or eBioscience).

Cell death assays

For demonstration of DNA fragmentation, TUNEL staining was performed according to the manufacturer's instructions (in situ cell death detection kit, TMR red or FITC; Roche) and quantified in vitro by counting TUNEL+ cells in at least eight randomly chosen vision fields of each slide at an original magnification of ×40 using confocal laser microscopy, as previously described (19). For detection of caspase-1 activation, live cells were stained with the caspase-1 protease assay kit with red fluorescence substrate (Origene) and Hoechst 33342 (Thermo Scientific) for nuclei, and immediately visualized by confocal laser microscopy.

Protein analysis by immunoblotting and cytokine array

Proteins were isolated from cultured myeloid cells in ice-cold M-PER Mammalian and from colonic tissue samples using the T-PER Tissue Protein Extraction Reagents (Thermo Scientific; supplemented with PhosSTOP Phosphatase and complete Mini protease inhibitor mixture tablets [Roche], and 2 mM PMSF "plus" [Roche]). Immunoblotting was performed as previously described (34). Blots were reprobed with anti-Gapdh, anti–β-actin, or anti-COX IV to confirm equal protein loading. Representative blots of at least two independent experiments are shown. Equalized between samples, 100–250 μg/cell culture supernatant or tissue homogenate (TissueRuptor; Qiagen) were assayed in duplicate using mouse Ab arrays (#3 [62 cytokines] or #6 [97 cytokines]) from RayBiotech. Autoradiography films of array dots were scanned and converted to densitometric units using National Institutes of Health ImageJ software. Data were calculated using the RayBio Murine Cytokine Analysis Tool.

RNA/DNA extraction

Total RNA from murine terminal ileum or middle colon was extracted (RiboPure; Ambion) and purified including the RNase-free DNase digestion step (RNeasy Mini Kit; Qiagen). Total RNA and DNA from human colonic biopsies were isolated using the AllPrep Micro Kit (Qiagen). Genomic DNA from stool (cecum and large intestine) was isolated using the QIAmp DNA Stool Mini Kit including the high-temperature step.

Real-time PCR for murine gene expression analysis

QuantiTect Primer Assays (Qiagen) were used as the gene-specific murine primer pairs. The IL-10 primer was 5′-CGGGAAGACAATAACTG-3′ and 5′-CATTTCCGATAAGGCTTGG-3′ (35). Quantitative real-time RT-PCR was performed using the one-step QuantiFast SYBR Green RT-PCR kit (Qiagen) on the Mastercycler ep realplex (Eppendorf) real-time amplification system. Copy numbers of individual transcripts were related to Gapdh as endogenous control (×/100,000 copies Gapdh) and normalized against WT normal tissues, or as indicated.

Quantitative PCR for microbiota analysis

The abundance of specific intestinal bacterial groups was measured by quantitative PCR using the MyiQ Single-Color Real-Time PCR Detection System (BioRad) using group-specific 16S rDNA primers (Operon Technologies) as previously described (28). In brief, a short segment of the 16S rRNA gene (174 bp) was specifically amplified using the conserved 16S rRNA-specific primer pair UniF340 and UniR514 (IQ SYBR Green Supermix; BioRad) to determine the total amount of bacteria. Using genomic DNA from each sample, we completed real-time PCRs using group-specific primers (listed in Ref. 28) to determine the amount of bacteria in each of the following major groups: *Eubacterium rectale-Clostridium coccoides* (Erec), *Lactobacillus* sp. (Lact), *Bacteroides* sp. (Bact), *Mouse Intestinal Bacteroides* (MIB), and *Segmented Filamentous Bacteria* (SFB). Bacterial numbers were determined using standard curves constructed with plasmids containing the 16S sequence from reference bacterial DNA specific for each bacterial group analyzed.

RFLP

The genomic regions surrounding TLR2-R753Q and MDR1-C3435T were amplified with the following primers (36, 37): rs5743708, 5′-TATGGTC-CAGGAGCTGGAGA-3′ and 5′-TGACATAAAGATCCCAACTAGA-CAA-3′; and rs1045642, 5′-GTTTTCAGCTGC TTGATGGC-3′ and 5′-CATTAGGCAGTGACTCGATG-3′, respectively. The resulting amplicon was digested with SfcI or MboI (New England Biolabs), respectively, and separated by electrophoresis through an agarose gel.

Statistical analysis

The unpaired *t* test was used to calculate differences between means (GraphPad Prism version 5.04; GraphPad Software). All tests were two-tailed, and *p* values <0.05 were considered to be significant. All data are expressed as the means ± SEM.

Results

Deletion of TLR2 exacerbates development of spontaneous colitis in MDR1A KO mice

Initial studies revealed that TLR2 mRNA expression, but not TLR1/4/5/6, was selectively upregulated in inflamed MDR1A-deficient colons when compared with WT controls (Supplemental Fig. 1A). Although TLR9 mRNA was increased in MDR1A KO colitis, the overall expression level was negligible. To investigate the functional role of TLR2 in regulation of colitis pathogenesis in the context of MDR1A deficiency, mice double deficient in TLR2 and MDR1A and matched controls were generated in the FVB/N-background, as described in *Materials and Methods*. By the age of 5 wk, the TLR2/MDR1A dKO mice exhibited histologic evidence of colonic inflammation with a mean score of 3.2 (Fig. 1A, 1B). This was significantly greater than the mean score (∼1.5) for MDR1A KO controls, which all showed relatively normal intestinal architectures at this early stage (consistent with Refs. 8, 12). TLR2 KO controls were comparable with healthy WT. Microscopic inflammation in TLR2/MDR1A dKO was characterized by thickening of the mucosa and evidence of inflammatory cell infiltrates in the lamina propria, which were not present in MDR1A KO colons. However, the spleen was often enlarged regardless of the genotype (Fig. 1C). Levels of mRNA for TH1 cytokines IL-1β, IL-12p40, and IFN-γ (Fig. 1D)

week 5
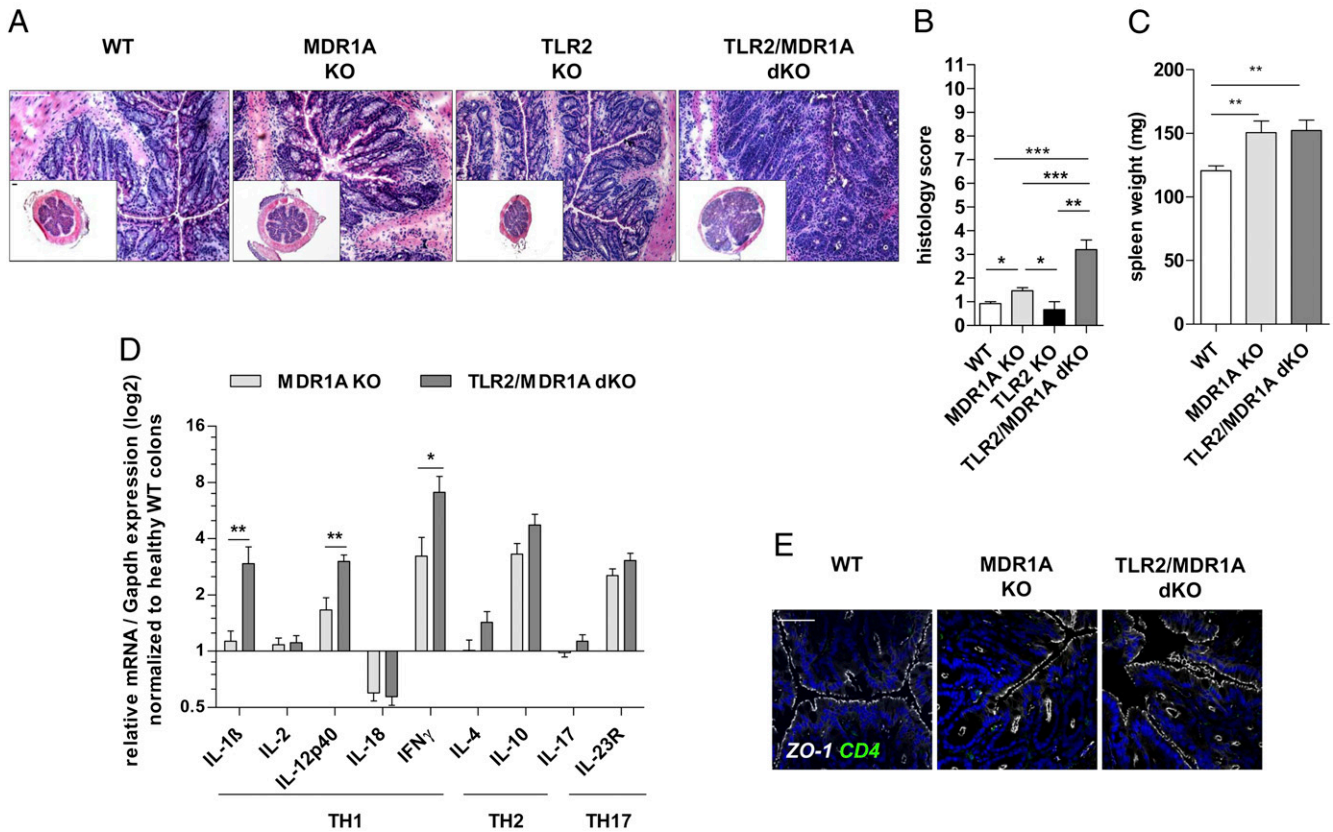
FIGURE 1. Deletion of TLR2 exacerbates chronic colitis development in MDR1A KO mice. Male WT (n = 5–6), MDR1A KO (n = 12), TLR2 KO (n = 3), and TLR2/MDR1A dKO (n = 10) mice were examined at 5 wk of age. (**A**) Representative distal colonic cross sections (H&E staining; scale bars, 100 μm) with (**B**) histology scores. (**C**) Spleen weight. (**D**) Relative expression of TH1/TH2/TH17 cytokine genes that were differentially regulated in middle colon samples, as determined by real-time RT-PCR analysis. Results (log2 base) are shown in relation to mRNA expression for the housekeeping gene *Gapdh* and normalized to the average expression levels of WT colons. Data are presented as means ± SEM. *p < 0.05, **p < 0.01, ***p < 0.001. (**E**) Representative morphology of intestinal epithelial ZO-1 (Cy5, white) before onset of colonic inflammation (histology score ≤ 2.5) in mice (n = 3/group), as assessed by confocal laser microscopy (scale bar, 50 μm). Cells were counterstained with DAPI for nuclei (blue) and anti-CD4 (FITC, green). Pooled or representative data from at least two independent experiments are shown.

were significantly elevated in TLR2/MDR1A dKO colons at 5 wk, when compared with MDR1A KO, indicating a relative TH1 skewing of the accelerated inflammatory response in the absence of TLR2. In contrast, there was no significant difference in expression of mRNA of TH2 or TH17 cytokines. Of note, both groups contained equally high expression of colonic IL-10 mRNA. In parallel, several increases of cytokines and chemokines associated with TH1 polarization and tissue damage were detectable by protein array in TLR2/MDR1A dKO colonic tissues (Supplemental Table I). This indicates that deletion of TLR2 leads to an exacerbated TH1 cytokine-associated form of colitis in MDR1A deficiency with earlier onset and higher incidence.

We have previously shown that ZO-1 mRNA and protein are downregulated in colitic MDR1A KO IEC (12). However, before onset of microscopic colitis, labeling of ZO-1 staining revealed normal expression and localization in MDR1A KO and TLR2/MDR1A dKO IEC (Fig. 1E), implying that exacerbation of colitis in TLR2/MDR1A dKO mice may not result from a primary defect in ZO-1–associated IEC barrier function. Once inflammatory cells infiltrated the lamina propria, focal ZO-1–associated defects in frontline enterocytes were comparable in both MDR1A-deficient groups (data not shown). We also considered that loss of TLR2 may lead to a selective defect in goblet cell–derived TFF3 production (19). However, TFF3 mRNA was reduced in both 5-wk-old MDR1A KO and TLR2/MDR1A dKO colons, and no differ-

ence was noted in the presence or absence of TLR2 (data not shown).

MyD88 is essential for the initiation of colitis in MDR1A KO mice models

By the age of 10 wk, most TLR2/MDR1A dKO mice developed fulminant pancolitis with associated loose stools (Fig. 2A, 2B). Histopathologic assessment showed massive thickening of the mucosa along the entire length of the colon, multiple crypt abscesses, loss of goblet cells, and evidence of large mucosal and submucosal leukocytic inflammatory infiltrates (Fig. 2A). This severe disease in TLR2/MDR1A dKO mice was associated with shortening of the colon, frequent adhesion to neighboring tissues, massive enlargement of spleen (Fig. 2C), and mesenteric lymph nodes and inflammatory infiltration to the liver (data not shown). In contrast, colitis in 10-wk-old MDR1A KO mice was much milder (Fig. 2A, 2B), and only a quarter of the animals developed severe disease, whereas WT and TLR2 KO controls did not exhibit any signs of colonic inflammation. Of note, neither TLR2/MDR1A dKO nor MDR1A KO mice developed rectal prolapse or showed intestinal bleeding. At this later stage of disease, mRNA of proinflammatory cytokines including IL-1β, IL-2, IL-12p40, IFN-γ, IL-17, and IL-23R was equally increased in the colons of TLR2/MDR1A dKO and MDR1A KO mice (Fig. 2D). Yet, enriched lamina propria T cells from TLR2/MDR1A dKO mice demonstrated baseline

week 10
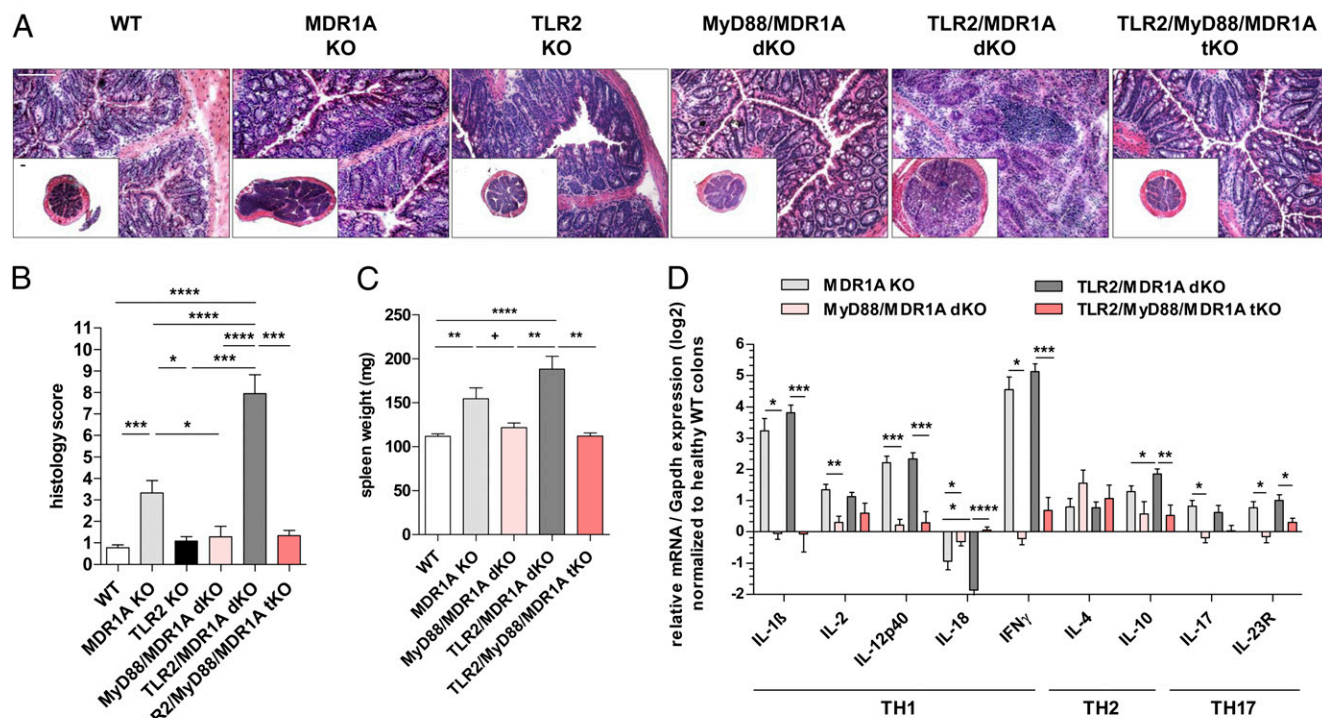
FIGURE 2. MyD88 is essential for the initiation of spontaneous colitis in MDR1A KO mice models. Male WT ($n = 20$), MDR1A KO ($n = 20$), TLR2 KO ($n = 6$), MyD88/MDR1A dKO ($n = 9$), TLR2/MDR1A dKO ($n = 18$), and TLR2/MyD88/MDR1A tKO ($n = 6$) mice were examined at 10 wk of age. (**A**) Representative distal colonic cross sections (H&E staining; scale bars, 100 μm) with (**B**) histology scores. (**C**) Spleen weight. (**D**) Relative expression of TH1/TH2/TH17 cytokine genes that were differentially regulated in middle colon samples, as determined by real-time RT-PCR analysis. Every two samples (equivalent histology scores) were pooled in the MDR1A KO and TLR2/MDR1A dKO groups, respectively. Results (log2 base) are shown in relation to mRNA expression for the housekeeping gene *Gapdh* and normalized to the average expression of WT colons. Pooled or representative data from at least two independent experiments are shown. Data are presented as means ± SEM. *$p < 0.05$, **$p < 0.01$, ***$p < 0.001$, ****$p < 0.0001$, +$p > 0.05$.

hyperreactivity that was reflected in increased amounts of cytokines and chemokines in the supernatant, when compared with MDR1A KO (Supplemental Table II).

Next, we assessed the role of MyD88, the major signaling adaptor molecule of the TLR and IL-1R families, in the induction of chronic colitis in MDR1A deficiency. Loss of MyD88 completely abolished all signs of colitis development in both MDR1A KO and TLR2/MDR1A dKO groups (Fig. 2A–C). Colons from 10-wk-old MyD88/MDR1A dKO and TLR2/MyD88/MDR1A tKO appeared healthy, mean histology scores resembled those of WT controls (Fig. 2A, 2B), and no splenomegaly was observed (Fig. 2C). The inflammatory TH1/TH2/TH17 cytokines were all nearly normal in both colonic groups relative to WT controls (Fig. 2D). These findings reveal an essential role for MyD88-dependent signaling receptors of inducing chronic colitis in the context of MDR1A and combined TLR2/MDR1A deficiencies.
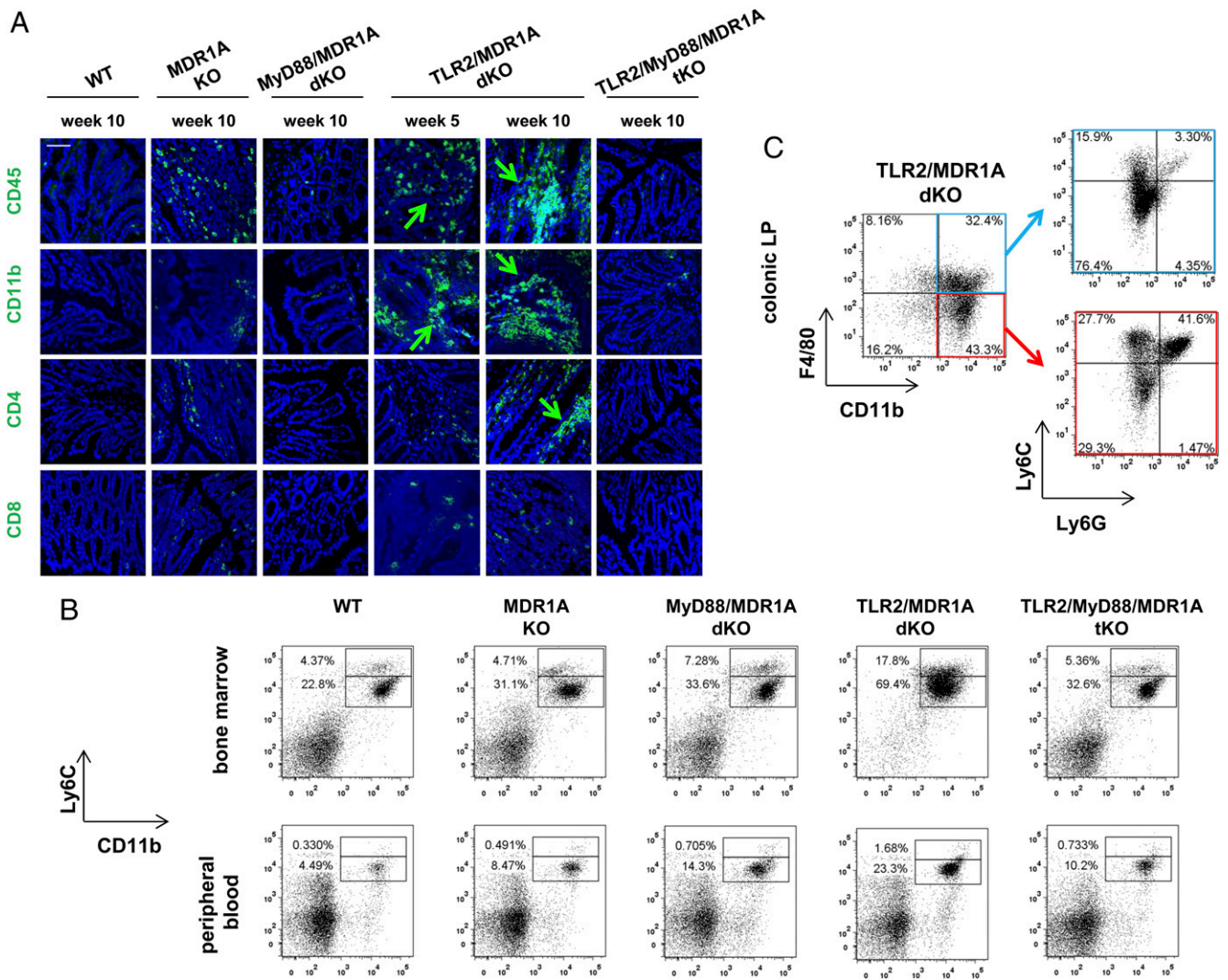
TLR2/MDR1A dKO mice have increased numbers of CD11b+ cells in bone marrow, peripheral blood, and colon

Next, we characterized the predominant cell type of the extensive inflammatory lamina propria infiltrates seen in severe TLR2/MDR1A dKO colitis. Immunohistochemical staining of 5-wk-old TLR2/MDR1A dKO colons demonstrated the early CD45+ cell infiltrates to mostly consist of increased numbers of myeloid CD11b+ cells and only few CD4+ T cells (Fig. 3A). By 10 wk, abundant CD11b+ clusters were recruited and the number of CD4+ T cells also increased in the TLR2/MDR1A dKO lamina propria. In contrast, just a few scattered CD11b+ cells were present in the lamina propria of MDR1A KO, but absent in the lamina propria of TLR2/MyD88/MDR1A tKO. We defined the populations of CD11b+ leukocytes associated with colitis in TLR2/MDR1A dKO mice. Quantitatively, the overall numbers of CD11b+Ly6C^{high} and CD11b+Ly6C^{low} cells in bone marrow and peripheral blood circulation were increased early in TLR2/MDR1A dKO mice, but not in any of the other genotypes (Fig. 3B), implying that chronic colitis exacerbation in TLR2/MDR1A dKO mice is associated with increased myelopoiesis. We identified four major colitis-associated CD11b+ cell populations in the colonic lamina propria of TLR2/MDR1A dKO mice (Fig. 3C): 1) CD11b+F4/80+Ly6C−Ly6G− (mature macrophages), 2) CD11b+F4/80+Ly6C+Ly6G− (immature macrophages), 3) CD11b+F4/80−Ly6C+Ly6G− (monocytes), and 4) CD11b+F4/80−Ly6C+Ly6G+ (granulocytes). Analysis of the tissue-resident CD11b+F4/80−Ly6C−Ly6G− cell subpopulation revealed a macrophage-like SSC^{low}CD11c−CD103− phenotype (data not shown) that may have lost expression of the macrophage marker F4/80 under inflammatory conditions, as previously described (38).

Expansion of TLR2/MDR1A dKO CD11b+ myeloid cells is mediated by gut commensals

To test whether the commensal microbiota are required for the severe myeloid cell–mediated disease process, TLR2/MDR1A dKO mice were given broad-spectrum antibiotics as prophylaxis or therapy. Both antibiotic treatment forms ameliorated colitis. None of the TLR2/MDR1A dKO mice receiving antibiotic prophylaxis experienced development of pancolitis (Fig. 4). The only abnormality observed was cecal enlargement commonly seen in mice

FIGURE 3. TLR2/MDR1A dKO mice have increased numbers of CD11b$^+$ cells in bone marrow, peripheral blood, and colonic lamina propria. (**A**) Representative immunofluorescent staining with anti-CD45, anti-CD11b, anti-CD4, and anti-CD8 (FITC, green) of distal colons from 5- or 10-wk-old WT, MDR1A KO, MyD88/MDR1A dKO, TLR2/MDR1A dKO, and TLR2/MyD88/MDR1A tKO mice ($n = 3$/group), as assessed by confocal laser microscopy (scale bar, 50 μm). Green arrows indicate positive cells. Nuclei were counterstained with DAPI (blue). (**B**) Flow cytometry of bone marrow and peripheral blood cells isolated from WT, MDR1A KO, MyD88/MDR1A dKO, TLR2/MDR1A dKO, and TLR2/MyD88/MDR1A tKO mice (6 wk old; except WT: 9 wk old; $n = 3$/group) stained with V450-conjugated anti-Ly6C and streptavidin-coupled FITC detecting biotinylated anti-CD11b. Representative dot plot presents the incidence of CD11b$^+$Ly6C$^+$ cells in the total population. (**C**) Flow cytometry of colonic lamina propria cells isolated from TLR2/MDR1A dKO (12 wk old; $n = 3$/group), purified with anti–CD11b-PE magnetic beads, and stained with anti–F4/80-allophycocyanin-eFluor 780, anti–Ly6G-FITC, and anti–Ly6C-V450. Representative dot plot shows the incidence of CD11b$^+$F4/80$^+$ versus CD11b$^+$F4/80$^-$ cells in the purified population (*left*) with further analysis based on surface expression of Ly6C and Ly6G (*right*). Experiments were repeated at least twice.

maintained under antibiotic-treated and germ-free conditions. Histopathologic examination (Fig. 4A) demonstrated that antibiotic prophylaxis completely prevented development of chronic colitis (comparable with healthy WT controls; Fig. 1A). In contrast, therapy with antibiotics abrogated ongoing active inflammation and reduced mucosal thickening, yet smaller inflammatory infiltrates persisted throughout the lamina propria. Splenomegaly was prevented by antibiotic prophylaxis, but not reversed by therapy (Fig. 4B). The increased proportion of monocytic and granulocytic lineages in bone marrow and peripheral blood was reduced by antibiotics (Fig. 4C), which was associated with lack of CD11b$^+$ myeloid cell recruitment to the lamina propria in both treatment groups (Fig. 4D). Consistent with the absence of myeloid cell–associated inflammation, analysis of cytokine gene expression in colons (Fig. 4E) revealed near-complete normality in the prophylaxis group. Antibiotic therapy selectively decreased colonic

IL-1β mRNA production, but gene expression of the proinflammatory cytokines IL-12p40, IFN-γ, and IL-23R remained elevated, correlating with persistence of mucosal CD4$^+$ T cell infiltration (Fig. 4D). Collectively, these results show that CD11b$^+$ myeloid cell propagation is commensally dependent in TLR2/MDR1A dKO mice.

We considered that colitis exacerbation in TLR2/MDR1A dKO mice could result from altered microbiota. Paneth cell α-defensins can regulate the composition of the microbiota (28). However, amounts of mRNA transcripts encoding Paneth cell effector molecules in TLR2/MDR1A dKO and their MDR1A KO counterparts were comparable (Supplemental Fig. 1B). Furthermore, quantitative analysis of the most common bacterial groups comprising the intestinal microbiota revealed equal total bacterial numbers (Supplemental Fig. 1C). A slight decrease in the *Bacteroides* group was noted in the cecum of TLR2/MDR1A dKO
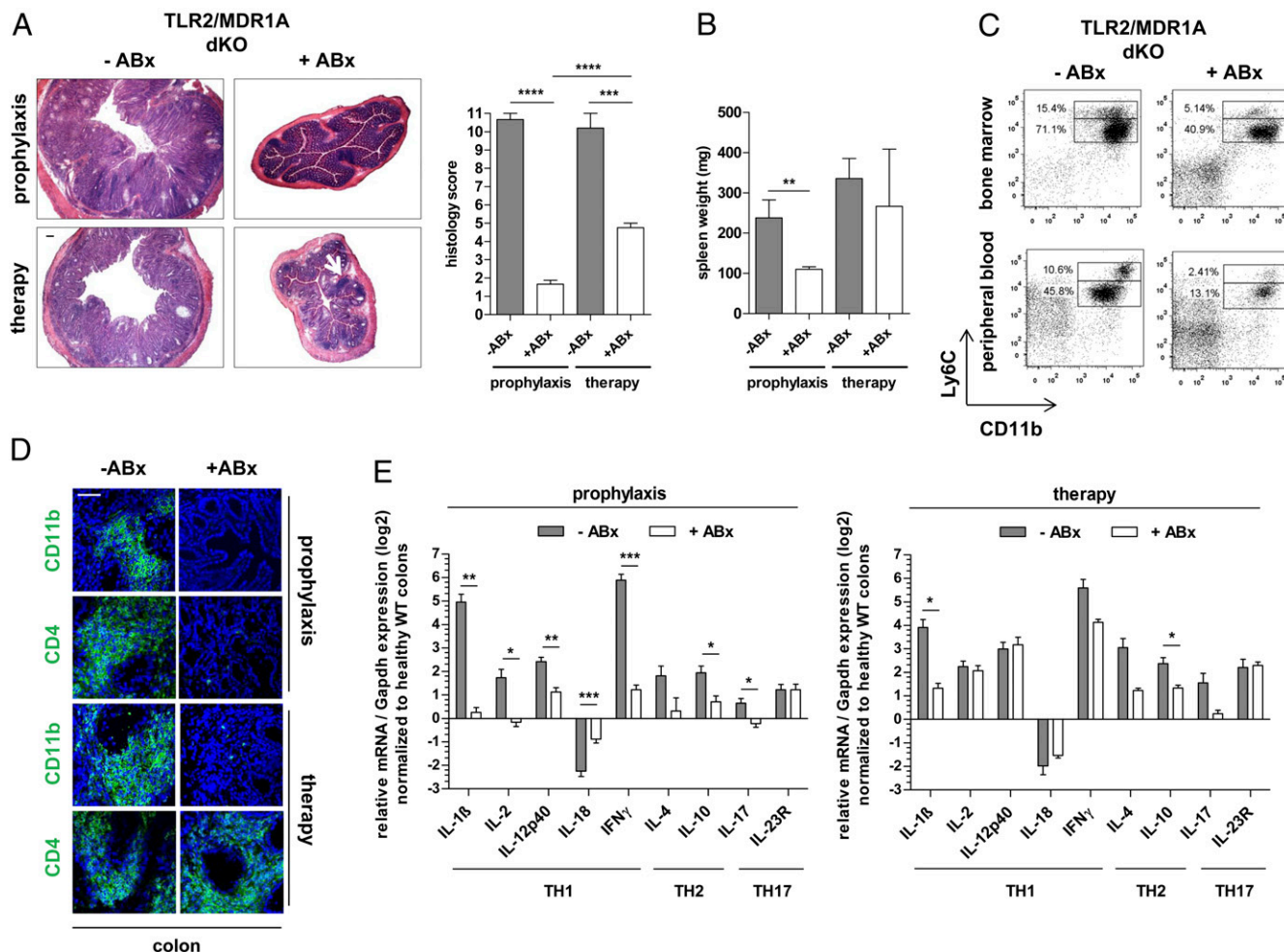
FIGURE 4. Expansion of TLR2/MDR1A dKO CD11b^{+} myeloid cells is mediated by gut commensals. TLR2/MDR1A dKO mice ($n = 4$–6) were treated prophylactically or therapeutically (+ABx) with oral broad-spectrum antibiotics (vancomycin/imipenem) for 8 wk and examined at the age of 11 or 26 wk, respectively. Control TLR2/MDR1A dKO mice ($n = 3$–5) were left untreated (−ABx). (**A**) Histology scores with representative distal colonic cross sections (H&E staining; scale bar, 100 μm; white arrow indicates lymphoid aggregates in lamina propria) and (**B**) spleen weight. (**C**) Representative flow cytometry analysis of bone marrow and peripheral blood cells isolated from control and prophylactic antibiotic-treated TLR2/MDR1A dKO mice ($n = 3$/group), stained with V450-conjugated anti-Ly6C and PE-Cy7–conjugated anti-CD11b. Dot plot presents the incidence of CD11b^{+}Ly6C^{+} cells in the total population. (**D**) Representative immunofluorescent staining with anti-CD11b and anti-CD4 (FITC, *green*) of distal TLR2/MDR1A dKO colons ($n = 3$/group) after antibiotic prophylaxis or therapy, as assessed by confocal laser microscopy (scale bar, 50 μm). Cells were counterstained with DAPI (blue). (**E**) Relative expression of TH1/TH2/TH17 cytokine genes that were differentially regulated in middle colon samples from TLR2/MDR1A dKO mice after antibiotic prophylaxis or therapy, as determined by real-time RT-PCR analysis. Results (log2 base) are shown in relation to mRNA expression for the housekeeping gene *Gapdh* and normalized to the average expression levels of WT colons. Data are presented as means ± SEM. *$p < 0.05$, **$p < 0.01$, ***$p < 0.001$, ****$p < 0.0001$.

mice when compared with MDR1A KO, but not in the large intestine. No other changes in the indigenous microbiota, including *Mouse Intestinal Bacteroides* and the *Segmented Filamentous Bacteria*, were detected. These data suggest that genetic manipulation of TLR2 in the context of MDR1A deficiency neither affects Paneth cell gene expression nor provokes major shifts in commensal composition.

MD-2 signaling is required for colitis acceleration in TLR2/MDR1A dKO mice

LPS from commensal Gram-negative bacteria, such as *E. coli*, is present in the normal gut and signals through MD-2/TLR4. As the number of MD-2/TLR4–expressing CD11b^{+} myeloid cells was significantly increased in TLR2/MDR1A dKO mice (Supplemental Fig. 2A), we hypothesized that commensal LPS hypersensitivity via MD-2/TLR4 may be responsible for the development of severe colitis in the context of TLR2/MDR1A double deficiency.

To test this, MDR1A KO mice lacking MD-2 and/or TLR2 were generated and their intestinal phenotype examined. Deletion of MD-2 in TLR2/MDR1A dKO mice significantly attenuated colitis progression (Fig. 5). TLR2/MD-2/MDR1A tKO mice only developed mild colitis without mucosal thickening and crypt abscesses, and lacked splenomegaly (Fig. 5A, 5B). The low mean histopathologic score of TLR2/MD-2/MDR1A tKO colons at the age of 10 wk was comparable with control MD-2/MDR1A dKO (Fig. 5A) and MDR1A KO (Fig. 2A). Analysis of colonic cytokine mRNA modulation (Fig. 5C) revealed that loss of MD-2 on a TLR2/MDR1A-null background significantly lowered upregulation of various proinflammatory cytokines, including IL-1β, IL-12p40, IFN-γ, and IL-23R. However, relative to WT controls, MD-2/MDR1A dKO and TLR2/MD-2/MDR1A tKO mice still had elevated gene expression of cytokines, which were comparable with MDR1A KO mice (Fig. 2D). These data suggest that baseline elevation of cytokines in MDR1A deficiency may be driven by another TLR-dependent, yet
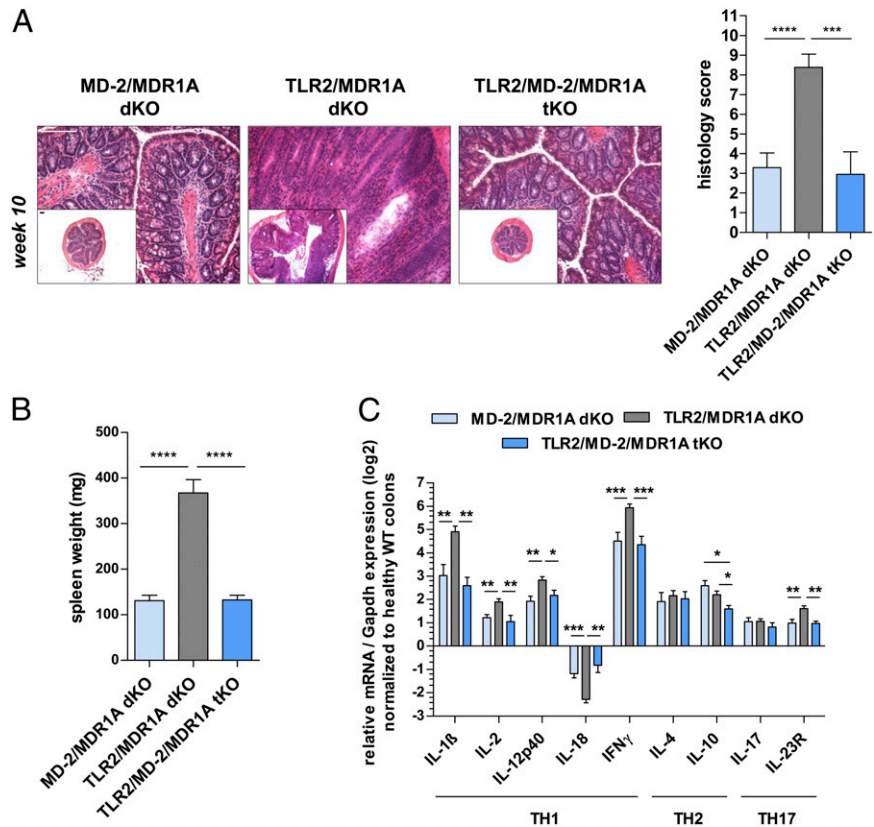
FIGURE 5. MD-2 signaling is required for colitis exacerbation in TLR2/MDR1A dKO mice. Male MD-2/MDR1A dKO ($n = 20$), TLR2/MDR1A dKO ($n = 13$), and TLR2/MD-2/MDR1A tKO ($n = 10$) mice were examined at 10 wk of age. (**A**) Histology scores with representative distal colonic cross sections (H&E staining; scale bars, 100 μm) and (**B**) spleen weight. (**C**) Relative expression of TH1/TH2/TH17 cytokine genes that were differentially regulated in middle colon samples, as determined by real-time RT-PCR analysis. Results (log2 base) are shown in relation to mRNA expression for the housekeeping gene *Gapdh* and normalized to the average expression in WT colons. Data are presented as means ± SEM. Pooled or representative data from at least two independent experiments are shown. *$p < 0.05$, **$p < 0.01$, ***$p < 0.001$, ****$p < 0.0001$.

MD-2-independent, pathway that functions upstream of MyD88 and remains to be identified. Collectively, these data imply that loss of TLR2 in MDR1A deficiency results in increased MD-2 activation and immune hyperresponsiveness to Gram-negative bacteria, which accelerated progression of colitis.
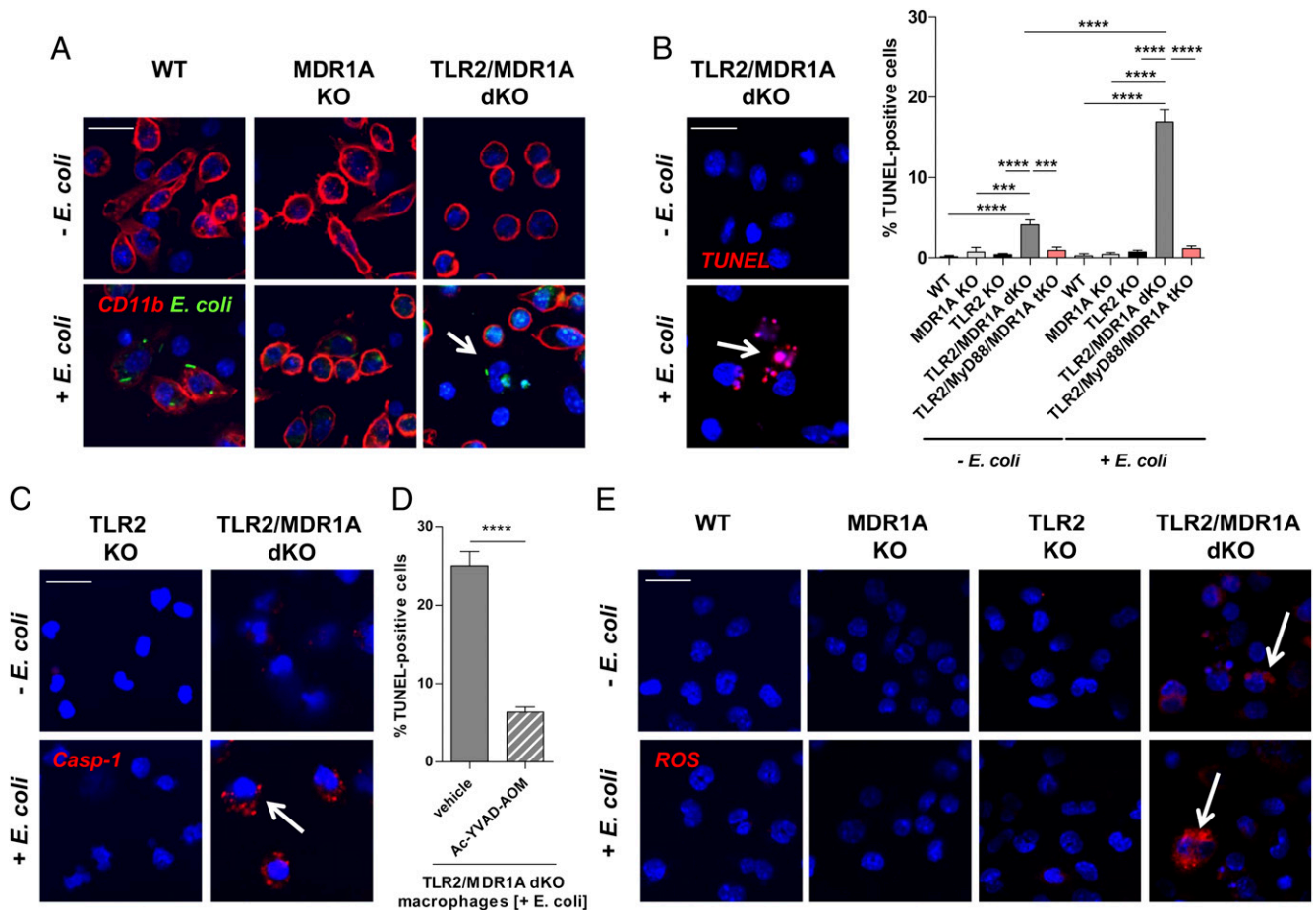
TLR2/MDR1A dKO CD11b^{+} myeloid cells respond to nonpathogenic E. coli *with caspase-1–dependent cell death*

Next, we tested how TLR2/MDR1A-deficient CD11b^{+} myeloid cells respond functionally to nonpathogenic *E. coli* (Fig. 6). Compared with WT or MDR1A KO, uptake of *E. coli*–enhanced GFP was unaffected by TLR2/MDR1A double deficiency in CD11b^{+} myeloid cells (Fig. 6A). Normal phagocytic activity was confirmed by quantitative analysis (Supplemental Fig. 2B). However, many TLR2/MDR1A dKO CD11b^{+} myeloid cells showed membrane rupture in response to intracellular *E. coli* already after 90 min of stimulation (Fig. 6A), which was not evident in TLR2-expressing MDR1A KO or WT. We found that CD11b^{+} peritoneal myeloid cells from TLR2/MDR1A dKO mice underwent markedly increased cell death in the presence of nonpathogenic *E. coli*, as assessed by nuclear morphology and DNA strand breaks using TUNEL assay (Fig. 6B). Some TLR2/MDR1A dKO CD11b^{+} myeloid cells already showed DNA fragmentation under baseline conditions without *E. coli* exposure. In contrast, increased cell death was not present in WT, MDR1A KO, or in TLR2 KO macrophages stimulated with nonpathogenic *E. coli*. Cell death was completely abolished in TLR2/MyD88/MDR1A tKO cells, implying that *E. coli*–induced cell death is MyD88 dependent in TLR2/MDR1A double deficiency. TUNEL staining of TLR2/MDR1A dKO CD11b^{+} myeloid cells after *E. coli* stimulation demonstrated "balloon-shaped" vesicles around the nucleus with absence of nuclear fragmentation, suggestive of pyroptosis (39). Live TLR2/MDR1A dKO myeloid cells showed increased caspase-1 activation upon *E. coli* exposure (Fig. 6C), and increased cell death was blocked by a specific caspase-1 inhibitor

(Fig. 6D). Increased ROS generation may induce inflammasome-mediated caspase-1 activation (40), thus triggering pyroptosis. We found that cell death was associated with enhanced ROS production in *E. coli*–stimulated TLR2/MDR1A dKO CD11b^{+} myeloid cells, which was not evident in WT, MDR1A KO, or TLR2 KO macrophages (Fig. 6E). Notably, intracellular ROS was already slightly elevated in baseline TLR2/MDR1A dKO CD11b^{+} myeloid cells. These data imply that TLR2/MDR1A dKO CD11b^{+} myeloid cells hyperrespond to nonpathogenic *E. coli* with excessive ROS activation and associated caspase-1–dependent cell death.

Disease exacerbation in TLR2/MDR1A dKO mice is induced by IL-1β

Pyroptosis is accompanied by caspase-1–dependent processing and release of the proinflammatory cytokine IL-1β. We have observed increased mRNA expression of IL-1β in TLR2/MDR1A dKO already at 5 wk of age, but not in MDR1A KO (Fig. 1C). Next, we confirmed that expression of IL-1β protein was selectively elevated in the lamina propria of TLR2/MDR1A dKO, but not in any of the other genotypes, including TLR2/MyD88/MDR1A tKO, implying an MyD88-dependent pathway (Fig. 7A). Production of IL-1β protein in TLR2/MDR1A dKO colons was commensally dependent, as both antibiotic prophylaxis and therapy completely blocked IL-1β synthesis (Fig. 7B). Stimulation of TLR2/MDR1A dKO myeloid cells with *E. coli* LPS led to increased production of pro–IL-1β and mature IL-1β (Fig. 7C), implying that cell death (Fig. 6B) is associated with a highly proinflammatory event, consistent with pyroptosis. WT or MDR1A KO myeloid cells did not show hyperresponsiveness to LPS, as synthesis of pro–IL-1β was not enhanced. Notably, stimulation with *E. coli* LPS induced production of pro–IL-18 similarly in all three genotypes, suggesting a specific LPS-mediated effect on IL-1β synthesis in the context of TLR2/MDR1A double deficiency. The contrasting decrease of IL-18 mRNA expression observed in colonic tissues may

FIGURE 6. TLR2/MDR1A dKO CD11b^{+} myeloid cells respond to commensal *E. coli* with caspase-1–dependent cell death. (**A**) Peritoneal myeloid cells from WT, MDR1A KO, and TLR2/MDR1A dKO mice were stimulated with or without *E. coli*–GFP (FITC, green) for 90 min and visualized with anti-CD11b (CY5, red) using confocal immunofluorescence (scale bar, 20 μm). Cells were counterstained with DAPI (blue) for nuclei. White arrow indicates cells with membrane rupture and nuclei fragmentation. (**B**) TUNEL (rhodamine, red) assay of peritoneal myeloid cells from WT, MDR1A KO, TLR2 KO, TLR2/MDR1A dKO, and TLR2/MyD88/MDR1A tKO mice with or without *E. coli* exposure for 90 min using confocal immunofluorescence (representative image of TLR2/MDR1A dKO myeloid cells; scale bar, 20 μm). Cells were counterstained with DAPI (blue) for nuclei. White arrow indicates cells showing TUNEL[+] "balloon-shaped" vesicles around the nucleus. (**C**) Live TLR2 KO and TLR2/MDR1A dKO peritoneal myeloid cells were stained with cell-permeable fluorogenic substrate to identify cells with active caspase-1 (caspase-1 protease assay, red) with or without *E. coli* exposure for 90 min and assessed by confocal immunofluorescence (scale bar, 20 μm). Cells were counterstained with Hoechst 33342 (blue) for nuclei. (**D**) TLR2/MDR1A dKO peritoneal myeloid cells were pretreated with a specific caspase-1 inhibitor (100 μM) or vehicle control (DMSO) for 3 h, exposed to *E. coli* for 90 min, and TUNEL was performed. (**E**) WT, MDR1A, TLR2 KO, and TLR2/MDR1A dKO peritoneal myeloid cells were stimulated with or without *E. coli* for 90 min, and ROS production was assessed by confocal immunofluorescence (scale bar, 20 μm) using CellRox (CY5, red). Cells were counterstained with DAPI (blue) for nuclei. Arrows indicate representative ROS[+] TLR2/MDR1A dKO cells. Pooled or representative data from duplicate experiments are shown. (B and D) Ratio of live/dead cells is shown; data are presented as means ± SEM. ***$p < 0.001$, ****$p < 0.0001$.

represent a compensatory mechanism (Fig. 1D, 2D). Intracellular IL-1β protein expression was mainly detected in CD11b^{+}Ly6C^{+}Ly6G^{−} monocytes in the lamina propria of TLR2/MDR1A dKO mice (Fig. 7D).

We then investigated the role of IL-1β in the pathogenesis of colitis aggravation in TLR2/MDR1A dKO mice by reducing IL-1β activity with IL-1Ra treatment. Histopathologic examination demonstrated that neutralization of IL-1β signaling with IL-1Ra blocked development of severe colonic inflammation with markedly fewer infiltrates in TLR2/MDR1A dKO mice (Fig. 7E). Blockade of IL-1β by IL-1Ra inhibited splenomegaly (data not shown) and mRNA upregulation of the T cell marker CD3 and IL-12p40 (Fig. 7F), implying that T cell expansion and associated IL-12p40 production is driven by IL-1β. Although mRNA elevation of IL-1β (and IFN-γ) was not affected (Fig. 7F), IL-1β protein production was markedly reduced, which paralleled decrease of CD11b recruitment (Fig. 7G). Collectively, these data suggest that commensally mediated, pyroptosis-associated IL-1β

release is responsible for colitis exacerbation in TLR2/MDR1A dKO mice.

Blockade of ROS-mediated lysosome degradation suppresses LPS-induced IL-1β production in TLR2/MDR1A double deficiency

LAMP-1 represents an important marker of lysosomal integrity and function (41). LAMP-1 protects the lysosome membrane against the intraorganelle acidic environment. We found that the amount of the lysosomal structural protein LAMP-1 was significantly decreased in baseline and *E. coli* LPS-stimulated TLR2/MDR1A dKO myeloid cells, when compared with WT or MDR1A KO (Fig. 8A), suggesting lysosomal damage in TLR2/MDR1A double deficiency. ROS activation can induce loss of lysosomal integrity and functional destabilization (42). Treatment with the ROS inhibitor DPI or the lysosomal acidification inhibitor CQ elevated LAMP-1 protein expression in TLR2/MDR1A dKO CD11b^{+} myeloid cells, which was associated with blockade of increased
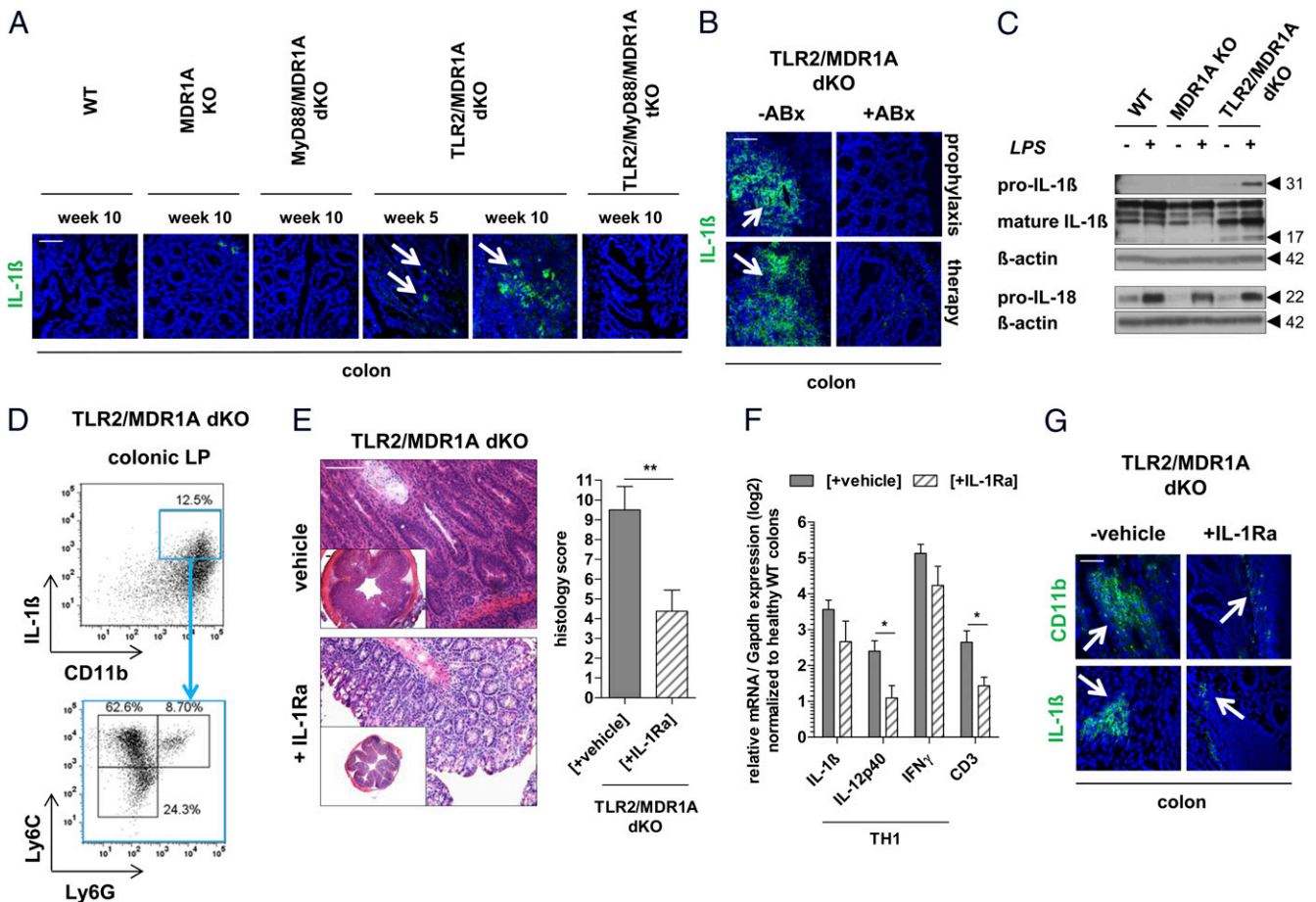
FIGURE 7. Disease exacerbation in TLR2/MDR1A dKO mice is induced by IL-1β. Representative immunofluorescent staining with anti–IL-1β (FITC, green) of distal colons (*n* = 3/group) from (**A**) 5- or 10-wk-old WT, MDR1A KO, MyD88/MDR1A dKO, TLR2/MDR1A dKO, and TLR2/MyD88/MDR1A tKO mice, and (**B**) TLR2/MDR1A dKO treated prophylactically or therapeutically with oral broad-spectrum antibiotics (ABx), as assessed by confocal laser microscopy (scale bars, 50 μm). (**C**) Assessment of pro–IL-1β, mature IL-1β, and pro–IL-18 protein synthesis in bone marrow–derived myeloid cells from WT, MDR1A KO, or TLR2/MDR1A dKO mice stimulated with *E. coli* LPS (1 μg/ml) for 23 h by Western blotting. Blots were reprobed with anti–β-actin to confirm equal loading. (**D**) Representative flow cytometry analysis of colonic lamina propria cells isolated from colitic TLR2/MDR1A dKO mice (*n* = 3/group), purified with anti–CD11b-PE magnetic beads, and stained with anti–IL-1β–allophycocyanin, anti–Ly6G-FITC, and anti–Ly6C-V450. Dot plot shows the incidence of CD11b^{+}IL-1β^{+} cells in the purified population (*upper panel*) with further analysis based on surface expression of Ly6C and Ly6G (*lower panel*). Experiments were repeated twice. (**E–G**) TLR2/MDR1A dKO mice (*n* = 7–8) were treated once daily by s.c. injection of IL-1Ra (100 mg/kg BW) or vehicle for 28 d. (E) Histology scores with representative distal colonic cross sections (H&E staining; scale bar, 100 μm). **$p < 0.01$. (F) Relative expression of selected TH1 cytokine genes that were differentially regulated in middle colon samples, as determined by real-time RT-PCR analysis. Results (log2 base) are shown in relation to mRNA expression for the housekeeping gene *Gapdh* and normalized to the average expression levels of WT colons. Data are presented as means ± SEM (*n* = 7–8). *$p < 0.05$. (G) Representative immunofluorescent staining with anti-CD11b and anti–IL-1β (FITC, green) of distal colons of TLR2/MDR1A dKO mice (*n* = 3/group) after treatment (scale bar, 50 μm).

IL-1β production in response to LPS stimulation (Fig. 8B). Treatment with the caspase-1 inhibitor Ac-YVAD-AOM or the inflammasome inhibitor GB also blocked LPS-induced IL-1β synthesis but had no influence on LAMP-1 depletion. These results imply that ROS-induced lysosome deregulation in the context of TLR2/MDR1A double deficiency may result in LPS hyperresponsiveness, thus driving colitis progression.

UC patients with TLR2/MDR1 *mutations show increased caspase-1 activation and cell death in the inflamed colonic lamina propria*

Finally, we investigated whether active UC patients with mutations in the *TLR2* and *MDR1* gene may show caspase-1–associated cell death in the lamina propria during colitis. We obtained samples from the inflamed colon of UC patients with active disease undergoing endoscopic examination (all with comparable disease activity; endoscopic Mayo score, 2–3). Nuclear translocation of caspase-1 protein indicates its activation (43). Immunohistochemistry revealed

increased nuclear expression of caspase-1 protein in the inflamed lamina propria of TLR2/MDR1-mutant active UC patients (Fig. 9), when compared with control active UC patients (MDR1-C3435T or WT). Of note, caspase-1 mRNA expression was significantly more upregulated in TLR2/MDR1-mutant UC patients than control UC (Supplemental Fig. 2C). Moreover, in the areas of caspase-1 activation, many more lamina propria mononuclear cells were TUNEL[+] in TLR2/MDR1-mutant UC patients compared with control UC patients (Fig. 9). Neither nuclear caspase-1 activity nor TUNEL[+] lamina propria mononuclear cells were observed in normal TLR2/MDR1-mutant or WT colonic tissues (data not shown). These data suggest that active UC in patients with TLR2/MDR1 mutations might be associated with features of pyroptosis during inflammation.

Discussion

Our results indicate that lack of TLR2-mediated signals leads to exacerbation of TH1-associated chronic intestinal inflammation in MDR1A deficiency. We demonstrate that commensally dependent
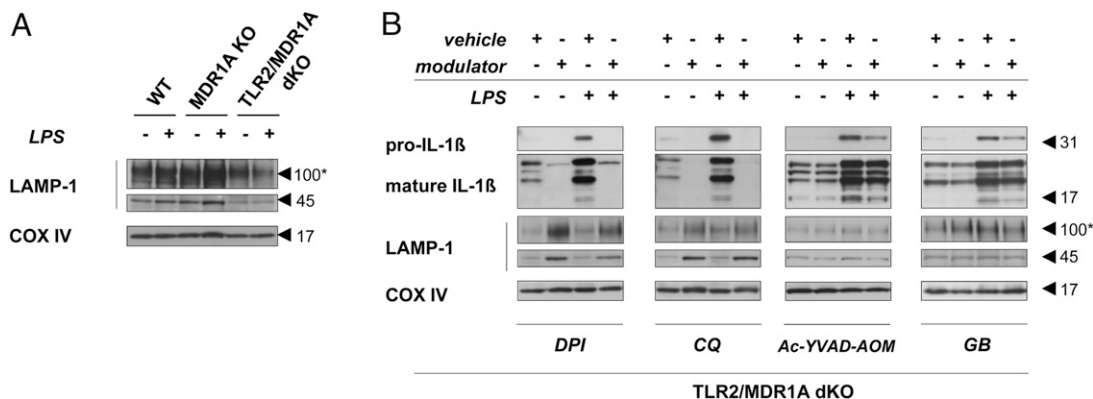
FIGURE 8. Inhibition of ROS-mediated lysosomal degradation is associated with suppression of LPS-induced, inflammasome-dependent IL-1β production in TLR2/MDR1A double deficiency. Assessment of pro–IL-1β, mature IL-1β, and/or LAMP-1 protein expression in bone marrow–derived myeloid cells isolated from (**A**) WT, MDR1A KO, and TLR2/MDR1A dKO mice or (**B**) TLR2/MDR1A dKO mice and stimulated with *E. coli* LPS (1 μg/ml) for up to 23 h by Western blotting. (B) Cells were pretreated with the following modulators: CQ (50 μM) for 1 h, DPI (20 μM) for 1 h, Ac-YVAD-AOM (100 μM) for 4 h, GB (50 μM) for 1 h, or corresponding vehicle (DMSO or water). Blots were reprobed with anti–COX IV to confirm equal loading. Asterisk indicates glycosylated form of LAMP-1.

colitis acceleration in TLR2/MDR1A dKO mice is caused by an exaggerated IL-1β–mediated immune response through MD-2 and IL-1R signaling via MyD88. Mechanistically, we identify pyroptosis as a maladaptive antimicrobial defense strategy caused by the combination of the two UC gene defects, which turns into a detrimental innate immune event against commensal bacteria, leading to early-onset and aggressive colitis.

Pyroptosis is an important innate effector mechanism that usually protects the host against intracellular pathogenic infections (44–46). Pyroptosis normally promotes pathogen clearance by acting as an alarm signal that recruits immune cells to the site of infection. It represents a form of caspase-1–dependent cell death characterized by cell lysis and inflammatory cytokine release that aims to limit the dissemination of intracellular pathogens. So far pyroptosis as an antibacterial response against nonpathogenic bacteria has not been described. In this article, we show that the combination of defects in two UC genes, *TLR2* and *MDR1A*, causes excessive cellular stress, including increased ROS generation, associated lysosomal damage, and caspase-1–dependent IL-1β production, leading to pyroptotic cell death in response to commensal *E. coli*. In contrast, TLR2-expressing MDR1A KO myeloid cells or MDR1A-expressing TLR2 KO myeloid cells lacked these features and survived after uptake of commensal *E. coli*, as normally seen in WT. Indeed, TLR2 KO mice did not show colitis development at all, whereas MDR1A KO mice developed only mild-to-moderate colitis, as previously described (8, 12), indicating that neither single-gene defect in TLR2 or MDR1A KO mice was sufficient to induce pyroptotic cell stress and cause fulminant pancolitis.

Pyroptosis is a highly proinflammatory event, because the proform of IL-1β is processed by inflammasome-dependent caspase-1 activation and released during cell death (44–46). We determined IL-1β as a central mediator of colitis progression and exacerbation in TLR2/MDR1A double deficiency. IL-1β expression was selectively upregulated in TLR2/MDR1A dKO colons. When compared with WT or MDR1A KO, exposure of TLR2/MDR1A dKO myeloid cells to *E. coli* LPS showed hypersensitivity and responded with abnormally high production of IL-1β, but not IL-18, suggesting a potential distinct mechanism of signaling regulation (47, 48). ROS production, which is required for the release of mature, fully processed IL-1β (49) and exerts antimicrobial activity, was increased in baseline and pyroptotic *E. coli*–stimulated TLR2/MDR1A dKO myeloid cells. Future studies will need to determine the molecular cause of intracellular ROS in the context of TLR2/MDR1A double deficiency. We

identified a small population of inflammatory monocytes as the main cellular source of IL-1β production in the lamina propria. Mature IL-1β may bind to the IL-1R present on local immune cells, causing extensive tissue damage and promoting myeloid cell infiltration and activation in an autocrine loop (50). T cells are a major target of IL-1β (51). Blockade of IL-1β activity by administration of IL-1Ra markedly reduced mucosal inflammation and associated IL-12 production in TLR2/MDR1A dKO colons. Of note, IL-1Ra also partially inhibited IL-1β protein synthesis, suggesting an autocrine loop via IL-1R. Taken together, our results imply that pyroptotic CD11b+-derived IL-1β is responsible for TH1-mediated colitis progression in our model. Previously, administration of IL-1Ra has also proved to be anti-inflammatory in a model of acute immune-complex colitis in rabbits (52). However, genetic studies using caspase-1−/− (47, 53)
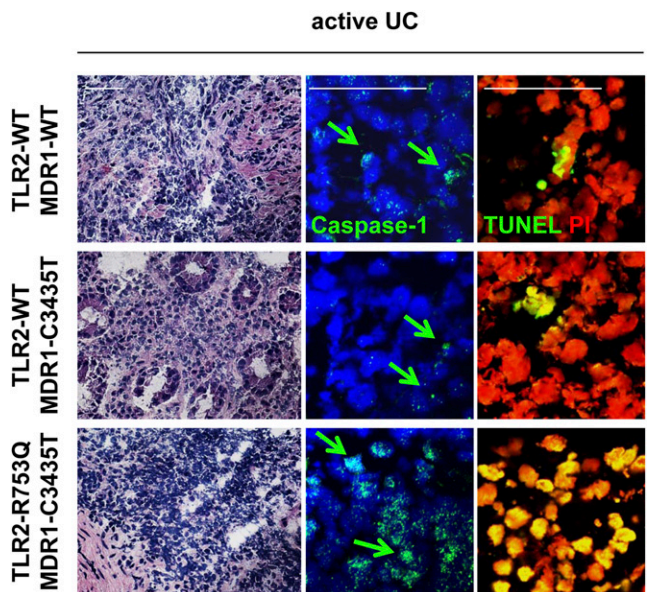
active UC

FIGURE 9. Caspase-1 protein expression and cell death are increased in human colonic lamina propria mononuclear cells of active UC patients carrying both TLR2-R753Q and MDR1-C3435T mutations. Representative H&E and immunofluorescent staining (scale bars, 50 μm) with anti–caspase-1 and TUNEL (FITC, green) of colonic tissue samples from active UC patients (*n* = 10) genotyped for TLR2-R753Q and MDR1-C3435T polymorphisms. Arrows indicate nuclear expression of caspase-1 protein.

and IL-1R1$^{-/-}$ mice (54) rather implied a protective role for the inflammasome and related IL-1β signaling in acute DSS colitis in mice. Thus, the outcome of the caspase-1/IL-1R pathway in intestinal inflammation may be pleiotropic, depending on the colitis model used. IL-1R blockade has emerged as a therapeutic strategy for an expanding number of autoinflammatory and autoimmune diseases in humans (50). However, so far no large clinical trial has been performed in human IBD. Our findings are in support of reconsidering and evaluating the effectiveness of IL-1Ra in IBD treatment, at least in a subset of UC patients.

Pyroptosis has been linked to xenophagy, that is, autophagy against intracellular pathogens. When xenophagy is inhibited, *Shigella*-infected cells may undergo cell death by caspase-1–dependent pyroptosis (55). Macrophages that completely lack autophagy exhibit elevated IL-1β production after stimulation with LPS (56), although increased cell death as a consequence has not been observed. On an individual level, both TLR2 and MDR1A could be functionally linked to xenophagy. Cells deficient in TLR2 show defective autophagic defense against intracellular *Listeria monocytogenes* (57). Loss of MDR1A may allow increased pathogen invasion (58), thus possibly overstraining the autophagic machinery. Autophagosomes fuse with lysosomes to efficiently kill the ingested microorganism. In this study, we found that combined loss of TLR2 and MDR1 led to ROS-mediated LAMP-1 degradation, implying lysosome dysfunction. In contrast, phagocytosis was not altered by absence of TLR2 and/or MDR1A. Future studies will need to determine how TLR2 and MDR1A may possibly cooperate in modulating the autophagy–lysosome pathway.

The inflammasome may be stimulated by the presence of microbial-associated products, ROS, and other danger/stress signals (59, 60). Our data imply that the intestinal microbiota are responsible for the initiation and perpetuation of severe colonic inflammation in TLR2/MDR1A dKO mice, as development of mucosal disease was prevented and ameliorated by prophylactic or therapeutic antibiotics, respectively. In TLR2/MDR1A dKO mice, the CD11b$^+$-myeloid cell recruitment and associated IL-1β inflammatory environment in the lamina propria were commensally dependent. However, once chronic inflammation progressed, late intervention with antibiotics did not inhibit continuous CD4$^+$ T cell stimulation, only partially alleviating disease severity. We excluded abnormal microbial colonization in our mice strains that could have subverted the mucosal innate immune system.

MD-2 is an accessory protein of TLR4, essential for assembling a functional receptor complex to sense low concentrations of LPS. Soluble MD-2 may act as an acute-phase reactant in sepsis (61). Expression of MD-2 protein is significantly increased in the inflamed intestinal mucosa of patients with active IBD colitis (62). Here the exaggerated inflammatory response seen in TLR2/MDR1A double deficiency resulted from broken tolerance to commensal LPS via MD-2, as deletion of MD-2 markedly abrogated colitis exacerbation. However, development of colitis itself was not blocked in MD-2/MDR1A dKO mice, implying that MD-2 signaling is required for the progression but not for the initiation of colitis in MDR1A deficiency. Notably, others have recently shown that LPS signaling via TLR4 protects against acute DSS colitis (63, 64) and chronic colitis in IL-10–null mice (65, 66). Thus, LPS signaling can be either protective or destructive in the intestinal mucosa, depending on the genetic context.

MyD88 serves as the common adaptor protein at the level of TLR- and IL-1R–signaling pathways (27, 67). We show that intestinal pathology was completely dependent on MyD88 in MDR1A and TLR2/MDR1A deficiencies. MyD88 signaling was required for enhanced myeloid cell recruitment and pyroptotic cell death in TLR2/MDR1A dKO. Deletion of MyD88 prevented the induction

of early TH1 and late TH2/TH17 cytokines in the lamina propria. Because IL-1β synthesis was abolished in TLR2/MyD88/MDR1A tKO mice, our data suggest that IL-1β production is MyD88 dependent. Collectively, our findings imply that both MyD88-dependent pathways, MD-2 and IL-1R, are required for amplification of commensally dependent intestinal inflammation via IL-1β, driving a self-reinforcing cycle in TLR2/MDR1A double deficiency.

Finally, our findings indicate that active UC in patients with mutations in TLR2 and MDR1 may be associated with increased activation of caspase-1 and cell death in areas of acute inflammation, suggesting that pyroptosis could be involved in the pathogenesis of severe human UC. In conclusion, our data uncover an unexpected combinatory function of the two UC genes *TLR2* and *MDR1A* in controlling the commensally induced inflammatory immune response in myeloid cells and in regulating gut homeostasis. Commensally induced inflammatory cell death resulted in enhanced recruitment and prolonged immune cell activation in a feed-forward loop, thus amplifying colitis in the context of TLR2/MDR1A double deficiency. Targeting pyroptotic cellular mechanisms as well as related MD-2 and IL-1R signaling pathways via MyD88 may represent a promising therapeutic strategy in this subset of human IBD patients.

Disclosures

The authors have no financial conflicts of interest.

References

1. Xavier, R. J., and D. K. Podolsky. 2007. Unravelling the pathogenesis of inflammatory bowel disease. *Nature* 448: 427–434.
2. Abraham, C., and R. Medzhitov. 2011. Interactions between the host innate immune system and microbes in inflammatory bowel disease. *Gastroenterology* 140: 1729–1737.
3. Sartor, R. B. 2008. Microbial influences in inflammatory bowel diseases. *Gastroenterology* 134: 577–594.
4. Schwab, M., E. Schaeffeler, C. Marx, M. F. Fromm, B. Kaskas, J. Metzler, E. Stange, H. Herfarth, J. Schoelmerich, M. Gregor, et al. 2003. Association between the C3435T MDR1 gene polymorphism and susceptibility for ulcerative colitis. *Gastroenterology* 124: 26–33.
5. Ho, G. T., E. R. Nimmo, A. Tenesa, J. Fennell, H. Drummond, C. Mowat, I. D. Arnott, and J. Satsangi. 2005. Allelic variations of the multidrug resistance gene determine susceptibility and disease behavior in ulcerative colitis. *Gastroenterology* 128: 288–296.
6. Blokzijl, H., S. Vander Borght, L. I. Bok, L. Libbrecht, M. Geuken, F. A. van den Heuvel, G. Dijkstra, T. A. Roskams, H. Moshage, P. L. Jansen, and K. N. Faber. 2007. Decreased P-glycoprotein (P-gp/MDR1) expression in inflamed human intestinal epithelium is independent of PXR protein levels. *Inflamm. Bowel Dis.* 13: 710–720.
7. Schinkel, A. H., J. J. Smit, O. van Tellingen, J. H. Beijnen, E. Wagenaar, L. van Deemter, C. A. Mol, M. A. van der Valk, E. C. Robanus-Maandag, H. P. te Riele, et al. 1994. Disruption of the mouse mdr1a P-glycoprotein gene leads to a deficiency in the blood-brain barrier and to increased sensitivity to drugs. *Cell* 77: 491–502.
8. Panwala, C. M., J. C. Jones, and J. L. Viney. 1998. A novel model of inflammatory bowel disease: mice deficient for the multiple drug resistance gene, mdr1a, spontaneously develop colitis. *J. Immunol.* 161: 5733–5744.
9. Siccardi, D., K. L. Mumy, D. M. Wall, J. D. Bien, and B. A. McCormick. 2008. *Salmonella enterica* serovar Typhimurium modulates P-glycoprotein in the intestinal epithelium. *Am. J. Physiol. Gastrointest. Liver Physiol.* 294: G1392–G1400.
10. Maggio-Price, L., H. Bielefeldt-Ohmann, P. Treuting, B. M. Iritani, W. Zeng, A. Nicks, M. Tsang, D. Shows, P. Morrissey, and J. L. Viney. 2005. Dual infection with *Helicobacter bilis* and *Helicobacter hepaticus* in p-glycoprotein-deficient mdr1a$^{-/-}$ mice results in colitis that progresses to dysplasia. *Am. J. Pathol.* 166: 1793–1806.
11. Resta-Lenert, S., J. Smitham, and K. E. Barrett. 2005. Epithelial dysfunction associated with the development of colitis in conventionally housed mdr1a$^{-/-}$ mice. *Am. J. Physiol. Gastrointest. Liver Physiol.* 289: G153–G162.
12. Ey, B., A. Eyking, G. Gerken, D. K. Podolsky, and E. Cario. 2009. TLR2 mediates gap junctional intercellular communication through connexin-43 in intestinal epithelial barrier injury. *J. Biol. Chem.* 284: 22332–22343.
13. Fort, M. M., A. Mozaffarian, A. G. Stöver, Jda. S. Correia, D. A. Johnson, R. T. Crane, R. J. Ulevitch, D. H. Persing, H. Bielefeldt-Ohmann, P. Probst, et al.

2005. A synthetic TLR4 antagonist has anti-inflammatory effects in two murine models of inflammatory bowel disease. *J. Immunol.* 174: 6416–6423.

14. Cario, E. 2010. Toll-like receptors in inflammatory bowel diseases: a decade later. *Inflamm. Bowel Dis.* 16: 1583–1597.

15. Kawai, T., and S. Akira. 2011. Toll-like receptors and their crosstalk with other innate receptors in infection and immunity. *Immunity* 34: 637–650.

16. Jin, M. S., S. E. Kim, J. Y. Heo, M. E. Lee, H. M. Kim, S. G. Paik, H. Lee, and J. O. Lee. 2007. Crystal structure of the TLR1-TLR2 heterodimer induced by binding of a tri-acylated lipopeptide. *Cell* 130: 1071–1082.

17. Nagai, Y., S. Akashi, M. Nagafuku, M. Ogata, Y. Iwakura, S. Akira, T. Kitamura, A. Kosugi, M. Kimoto, and K. Miyake. 2002. Essential role of MD-2 in LPS responsiveness and TLR4 distribution. *Nat. Immunol.* 3: 667–672.

18. Pierik, M., S. Joossens, K. Van Steen, N. Van Schuerbeek, R. Vlietinck, P. Rutgeerts, and S. Vermeire. 2006. Toll-like receptor-1, -2, and -6 polymorphisms influence disease extension in inflammatory bowel diseases. *Inflamm. Bowel Dis.* 12: 1–8.

19. Podolsky, D. K., G. Gerken, A. Eyking, and E. Cario. 2009. Colitis-associated variant of TLR2 causes impaired mucosal repair because of TFF3 deficiency. *Gastroenterology* 137: 209–220.

20. Cario, E., G. Gerken, and D. K. Podolsky. 2007. Toll-like receptor 2 controls mucosal inflammation by regulating epithelial barrier function. *Gastroenterology* 132: 1359–1374.

21. Watanabe, T., A. Kitani, P. J. Murray, Y. Wakatsuki, I. J. Fuss, and W. Strober. 2006. Nucleotide binding oligomerization domain 2 deficiency leads to dysregulated TLR2 signaling and induction of antigen-specific colitis. *Immunity* 25: 473–485.

22. Boulard, O., M. J. Asquith, F. Powrie, and K. J. Maloy. 2010. TLR2-independent induction and regulation of chronic intestinal inflammation. *Eur. J. Immunol.* 40: 516–524.

23. Pelegrin, P., and A. Surprenant. 2006. Pannexin-1 mediates large pore formation and interleukin-1beta release by the ATP-gated P2X7 receptor. *EMBO J.* 25: 5071–5082.

24. Bauernfeind, F., E. Bartok, A. Rieger, L. Franchi, G. Núñez, and V. Hornung. 2011. Cutting edge: reactive oxygen species inhibitors block priming, but not activation, of the NLRP3 inflammasome. *J. Immunol.* 187: 613–617.

25. Gonzalez-Noriega, A., J. H. Grubb, V. Talkad, and W. S. Sly. 1980. Chloroquine inhibits lysosomal enzyme pinocytosis and enhances lysosomal enzyme secretion by impairing receptor recycling. *J. Cell Biol.* 85: 839–852.

26. Lamkanfi, M., J. L. Mueller, A. C. Vitari, S. Misaghi, A. Fedorova, K. Deshayes, W. P. Lee, H. M. Hoffman, and V. M. Dixit. 2009. Glyburide inhibits the Cryopyrin/Nalp3 inflammasome. *J. Cell Biol.* 187: 61–70.

27. Kawai, T., O. Adachi, T. Ogawa, K. Takeda, and S. Akira. 1999. Unresponsiveness of MyD88-deficient mice to endotoxin. *Immunity* 11: 115–122.

28. Salzman, N. H., K. Hung, D. Haribhai, H. Chu, J. Karlsson-Sjöberg, E. Amir, P. Teggatz, M. Barman, M. Hayward, D. Eastwood, et al. 2010. Enteric defensins are essential regulators of intestinal microbial ecology. *Nat. Immunol.* 11: 76–83.

29. Hoentjen, F., H. J. Harmsen, H. Braat, C. D. Torrice, B. A. Mann, R. B. Sartor, and L. A. Dieleman. 2003. Antibiotics with a selective aerobic or anaerobic spectrum have different therapeutic activities in various regions of the colon in interleukin 10 gene deficient mice. *Gut* 52: 1721–1727.

30. Ehses, J. A., G. Lacraz, M. H. Giroix, F. Schmidlin, J. Coulaud, N. Kassis, J. C. Irminger, M. Kergoat, B. Portha, F. Homo-Delarche, and M. Y. Donath. 2009. IL-1 antagonism reduces hyperglycemia and tissue inflammation in the type 2 diabetic GK rat. *Proc. Natl. Acad. Sci. USA* 106: 13998–14003.

31. Göthert, J. R., S. E. Gustin, J. A. van Eekelen, U. Schmidt, M. A. Hall, S. M. Jane, A. R. Green, B. Göttgens, D. J. Izon, and C. G. Begley. 2004. Genetically tagging endothelial cells in vivo: bone marrow-derived cells do not contribute to tumor endothelium. *Blood* 104: 1769–1777.

32. Nguyen, D. D., M. H. Maillard, V. Cotta-de-Almeida, E. Mizoguchi, C. Klein, I. Fuss, C. Nagler, A. Mizoguchi, A. K. Bhan, and S. B. Snapper. 2007. Lymphocyte-dependent and Th2 cytokine-associated colitis in mice deficient in Wiskott-Aldrich syndrome protein. *Gastroenterology* 133: 1188–1197.

33. Berger, S. B., X. Romero, C. Ma, G. Wang, W. A. Faubion, E. Compeer, M. Keszei, L. Rameh, N. Wang, et al. 2010. SLAM is a microbial sensor that regulates bacterial phagosome functions in macrophages. *Nat. Immunol.* 11: 920–927.

34. Eyking, A., B. Ey, M. Rünzi, A. I. Roig, H. Reis, K. W. Schmid, G. Gerken, D. K. Podolsky, and E. Cario. 2011. Toll-like receptor 4 variant D299G induces features of neoplastic progression in Caco-2 intestinal cells and is associated with advanced human colon cancer. *Gastroenterology* 141: 2154–2165.

35. Svetić, A., F. D. Finkelman, Y. C. Jian, C. W. Dieffenbach, D. E. Scott, K. F. McCarthy, A. D. Steinberg, and W. C. Gause. 1991. Cytokine gene expression after in vivo primary immunization with goat antibody to mouse IgD antibody. *J. Immunol.* 147: 2391–2397.

36. Huang, M. 2005. Polymorphisms of the gene encoding multidrug resistance protein 1 in taiwanese. *J. Food Drug Anal.* 13: 112–117.

37. Liadaki, K., E. Petinaki, C. Skoulakis, P. Tsirevelou, D. Klapsa, A. E. Germenis, and M. Speletas. 2011. Toll-like receptor 4 gene (TLR4), but not TLR2, polymorphisms modify the risk of tonsillar disease due to *Streptococcus pyogenes* and *Haemophilus influenzae*. *Clin. Vaccine Immunol.* 18: 217–222.

38. Ezekowitz, R. A., and S. Gordon. 1982. Down-regulation of mannosyl receptor-mediated endocytosis and antigen F4/80 in bacillus Calmette-Guérin-activated mouse macrophages. Role of T lymphocytes and lymphokines. *J. Exp. Med.* 155: 1623–1637.

39. Labbé, K., and M. Saleh. 2008. Cell death in the host response to infection. *Cell Death Differ.* 15: 1339–1349.

40. Dostert, C., V. Pétrilli, R. Van Bruggen, C. Steele, B. T. Mossman, and J. Tschopp. 2008. Innate immune activation through Nalp3 inflammasome sensing of asbestos and silica. *Science* 320: 674–677.

41. Eskelinen, E. L. 2006. Roles of LAMP-1 and LAMP-2 in lysosome biogenesis and autophagy. *Mol. Aspects Med.* 27: 495–502.

42. Guicciardi, M. E., M. Leist, and G. J. Gores. 2004. Lysosomes in cell death. *Oncogene* 23: 2881–2890.

43. Mao, P. L., Y. Jiang, B. Y. Wee, and A. G. Porter. 1998. Activation of caspase-1 in the nucleus requires nuclear translocation of pro-caspase-1 mediated by its prodomain. *J. Biol. Chem.* 273: 23621–23624.

44. Bergsbaken, T., S. L. Fink, and B. T. Cookson. 2009. Pyroptosis: host cell death and inflammation. *Nat. Rev. Microbiol.* 7: 99–109.

45. Miao, E. A., I. A. Leaf, P. M. Treuting, D. P. Mao, M. Dors, A. Sarkar, S. E. Warren, M. D. Wewers, and A. Aderem. 2010. Caspase-1-induced pyroptosis is an innate immune effector mechanism against intracellular bacteria. *Nat. Immunol.* 11: 1136–1142.

46. Franchi, L., T. Eigenbrod, R. Muñoz-Planillo, and G. Nuñez. 2009. The inflammasome: a caspase-1-activation platform that regulates immune responses and disease pathogenesis. *Nat. Immunol.* 10: 241–247.

47. Zaki, M. H., K. L. Boyd, P. Vogel, M. B. Kastan, M. Lamkanfi, and T. D. Kanneganti. 2010. The NLRP3 inflammasome protects against loss of epithelial integrity and mortality during experimental colitis. *Immunity* 32: 379–391.

48. Schmidt, R. L., and L. L. Lenz. 2012. Distinct licensing of IL-18 and IL-1β secretion in response to NLRP3 inflammasome activation. *PLoS ONE* 7: e45186.

49. Tassi, S., S. Carta, L. Delfino, R. Caorsi, A. Martini, M. Gattorno, and A. Rubartelli. 2010. Altered redox state of monocytes from cryopyrin-associated periodic syndromes causes accelerated IL-1beta secretion. *Proc. Natl. Acad. Sci. USA* 107: 9789–9794.

50. Dinarello, C. A. 2009. Immunological and inflammatory functions of the interleukin-1 family. *Annu. Rev. Immunol.* 27: 519–550.

51. Ben-Sasson, S. Z., J. Hu-Li, J. Quiel, S. Cauchetaux, M. Ratner, I. Shapira, C. A. Dinarello, and W. E. Paul. 2009. IL-1 acts directly on CD4 T cells to enhance their antigen-driven expansion and differentiation. *Proc. Natl. Acad. Sci. USA* 106: 7119–7124.

52. Cominelli, F., C. C. Nast, A. Duchini, and M. Lee. 1992. Recombinant interleukin-1 receptor antagonist blocks the proinflammatory activity of endogenous interleukin-1 in rabbit immune colitis. *Gastroenterology* 103: 65–71.

53. Allen, I. C., E. M. TeKippe, R. M. Woodford, J. M. Uronis, E. K. Holl, A. B. Rogers, H. H. Herfarth, C. Jobin, and J. P. Ting. 2010. The NLRP3 inflammasome functions as a negative regulator of tumorigenesis during colitis-associated cancer. *J. Exp. Med.* 207: 1045–1056.

54. González-Navajas, J. M., J. Law, K. P. Nguyen, M. Bhargava, M. P. Corr, N. Varki, L. Eckmann, H. M. Hoffman, J. Lee, and E. Raz. 2010. Interleukin 1 receptor signaling regulates DUBA expression and facilitates Toll-like receptor 9-driven antiinflammatory cytokine production. *J. Exp. Med.* 207: 2799–2807.

55. Dupont, N., S. Lacas-Gervais, J. Bertout, I. Paz, B. Freche, G. T. Van Nhieu, F. G. van der Goot, P. J. Sansonetti, and F. Lafont. 2009. *Shigella* phagocytic vacuolar membrane remnants participate in the cellular response to pathogen invasion and are regulated by autophagy. *Cell Host Microbe* 6: 137–149.

56. Saitoh, T., N. Fujita, M. H. Jang, S. Uematsu, B. G. Yang, T. Satoh, H. Omori, T. Noda, N. Yamamoto, M. Komatsu, et al. 2008. Loss of the autophagy protein Atg16L1 enhances endotoxin-induced IL-1beta production. *Nature* 456: 264–268.

57. Anand, P. K., S. W. Tait, M. Lamkanfi, A. O. Amer, G. Nunez, G. Pagès, J. Pouysségur, M. A. McGargill, D. R. Green, and T. D. Kanneganti. 2011. TLR2 and RIP2 pathways mediate autophagy of *Listeria monocytogenes* via extracellular signal-regulated kinase (ERK) activation. *J. Biol. Chem.* 286: 42981–42991.

58. Neudeck, B. L., J. M. Loeb, N. G. Faith, and C. J. Czuprynski. 2004. Intestinal P glycoprotein acts as a natural defense mechanism against *Listeria monocytogenes*. *Infect. Immun.* 72: 3849–3854.

59. Sutterwala, F. S., Y. Ogura, M. Szczepanik, M. Lara-Tejero, G. S. Lichtenberger, E. P. Grant, J. Bertin, A. J. Coyle, J. E. Galán, P. W. Askenase, and R. A. Flavell. 2006. Critical role for NALP3/CIAS1/Cryopyrin in innate and adaptive immunity through its regulation of caspase-1. *Immunity* 24: 317–327.

60. Muruve, D. A., V. Pétrilli, A. K. Zaiss, L. R. White, S. A. Clark, P. J. Ross, R. J. Parks, and J. Tschopp. 2008. The inflammasome recognizes cytosolic microbial and host DNA and triggers an innate immune response. *Nature* 452: 103–107.

61. Pugin, J., S. Stern-Voeffray, B. Daubeuf, M. A. Matthay, G. Elson, and I. Dunn-Siegrist. 2004. Soluble MD-2 activity in plasma from patients with severe sepsis and septic shock. *Blood* 104: 4071–4079.

62. Cario, E., D. T. Golenbock, A. Visintin, M. Rünzi, G. Gerken, and D. K. Podolsky. 2006. Trypsin-sensitive modulation of intestinal epithelial MD-2 as mechanism of lipopolysaccharide tolerance. *J. Immunol.* 176: 4258–4266.

63. Rakoff-Nahoum, S., J. Paglino, F. Eslami-Varzaneh, S. Edberg, and R. Medzhitov. 2004. Recognition of commensal microflora by toll-like receptors is required for intestinal homeostasis. *Cell* 118: 229–241.

64. Fukata, M., K. S. Michelsen, R. Eri, L. S. Thomas, B. Hu, K. Lukasek, C. C. Nast, J. Lechago, R. Xu, Y. Naiki, et al. 2005. Toll-like receptor-4 is required for intestinal response to epithelial injury and limiting bacterial translocation in a murine model of acute colitis. *Am. J. Physiol. Gastrointest. Liver Physiol.* 288: G1055–G1065.

65. Matharu, K. S., E. Mizoguchi, C. A. Cotoner, D. D. Nguyen, B. Mingle, O. I. Iweala, M. E. McBee, A. T. Stefka, G. Prioult, K. M. Haigis, et al. 2009. Toll-like receptor 4-mediated regulation of spontaneous *Helicobacter*-dependent colitis in IL-10-deficient mice. *Gastroenterology* 137: 1380–1390.e1381–1383.

66. González-Navajas, J. M., S. Fine, J. Law, S. K. Datta, K. P. Nguyen, M. Yu, M. Corr, K. Katakura, L. Eckman, J. Lee, and E. Raz. 2010. TLR4 signaling in effector CD4+ T cells regulates TCR activation and experimental colitis in mice. *J. Clin. Invest.* 120: 570–581.

67. Adachi, O., T. Kawai, K. Takeda, M. Matsumoto, H. Tsutsui, M. Sakagami, K. Nakanishi, and S. Akira. 1998. Targeted disruption of the MyD88 gene results in loss of IL-1- and IL-18-mediated function. *Immunity* 9: 143–150.